Standard Problem Exercise No. 3

Model 2: Equipment Hatch Model

April 3-14, 2011

Herman Graves
Lili Akin
Robert Dameron, PE
Patrick Chang, PE

Sandia National Laboratories is a multi-program laboratory managed and operated by Sandia Corporation, a wholly owned subsidiary of Lockheed Martin Corporation, for the U.S. Department of Energy's National Nuclear Security Administration under contract DE-AC04-94AL85000.

Standard Problem Exercise No. 3 Summary

Model 2 continues examining:

- **Effects of containment dilation on prestressing force**
- **Slippage of prestressing cables**
- **Steel-concrete interface**
- **Fracture mechanics behavior**

MOFFATT & NICHOL
Sandia National Laboratories

Model 2 Summary

- **Detailed model of the Equipment Hatch**
- **In addition, studying the ovalization of concrete versus steel and the displacement and leakage this could cause**
- **Temperature analysis was not part of the SPE for Model 2**

Model 2 – Local E/H Model Geometry and Boundary Conditions

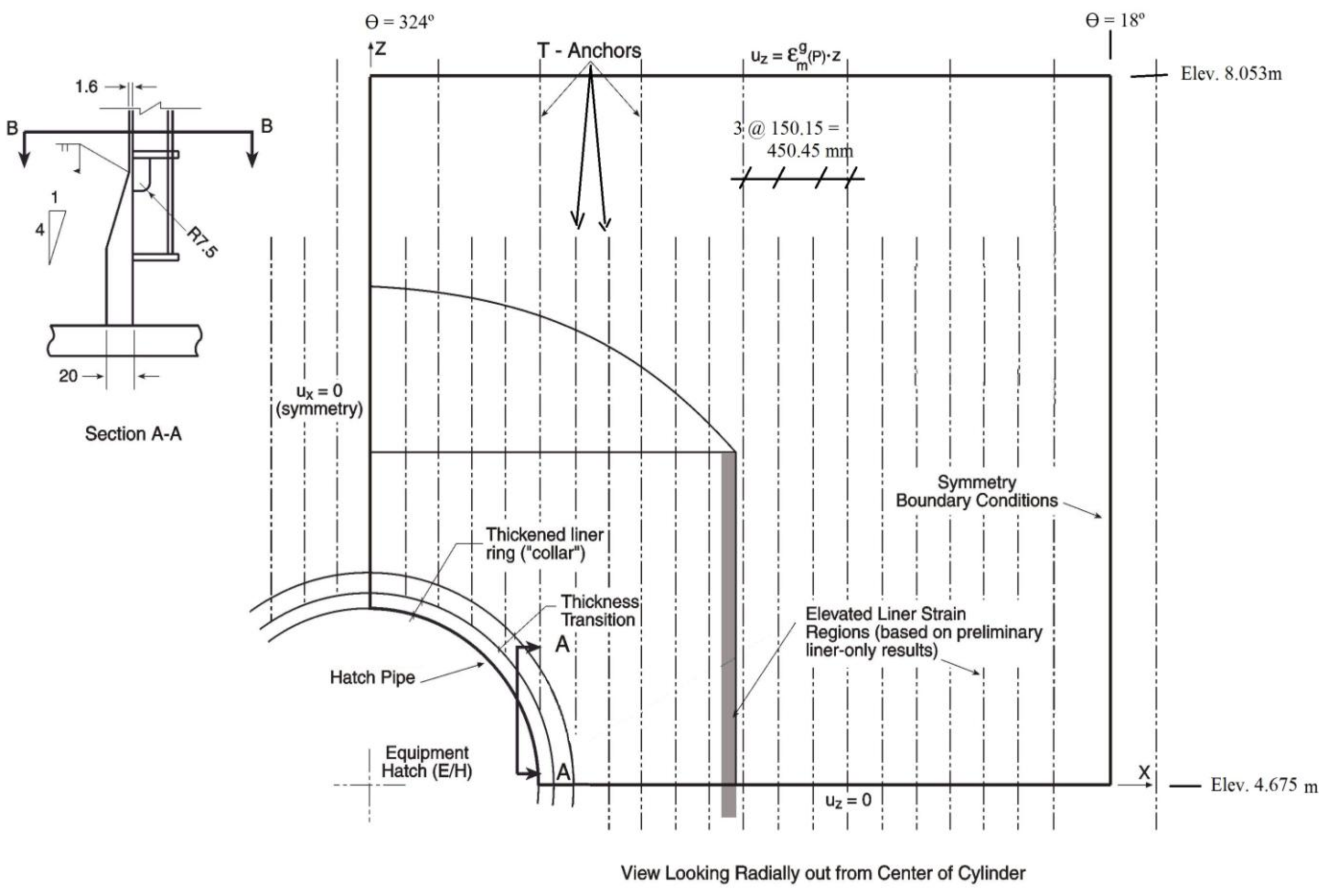

Detailed Liner Analysis Near E/H (View from Inside PCCV Looking Out Radially)

MOFFATT & NICHOL

Sandia National Laboratories

Model 2 – Perspective View

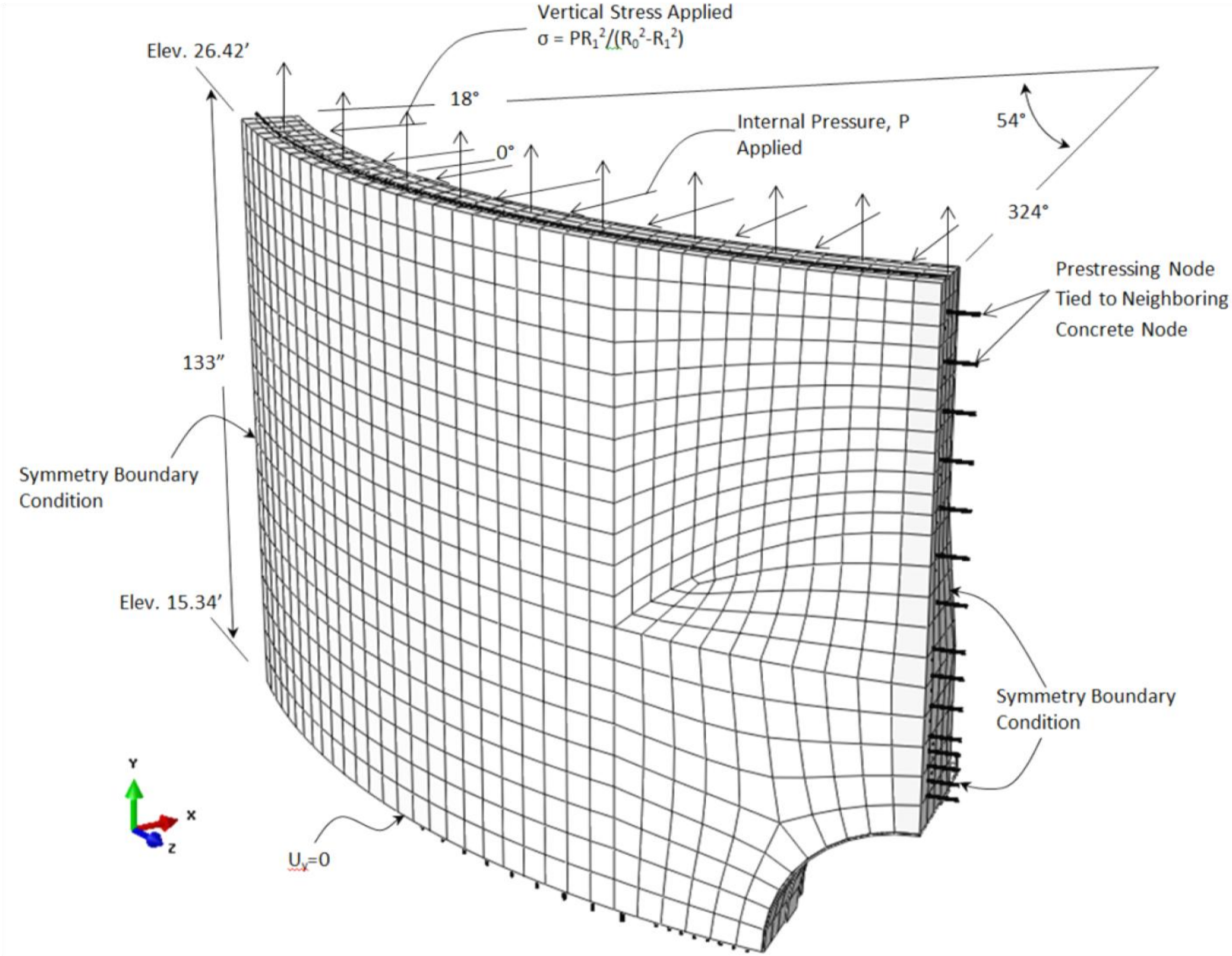

MOFFATT & NICHOL

Sandia National Laboratories

Rebar Summary for Model 2

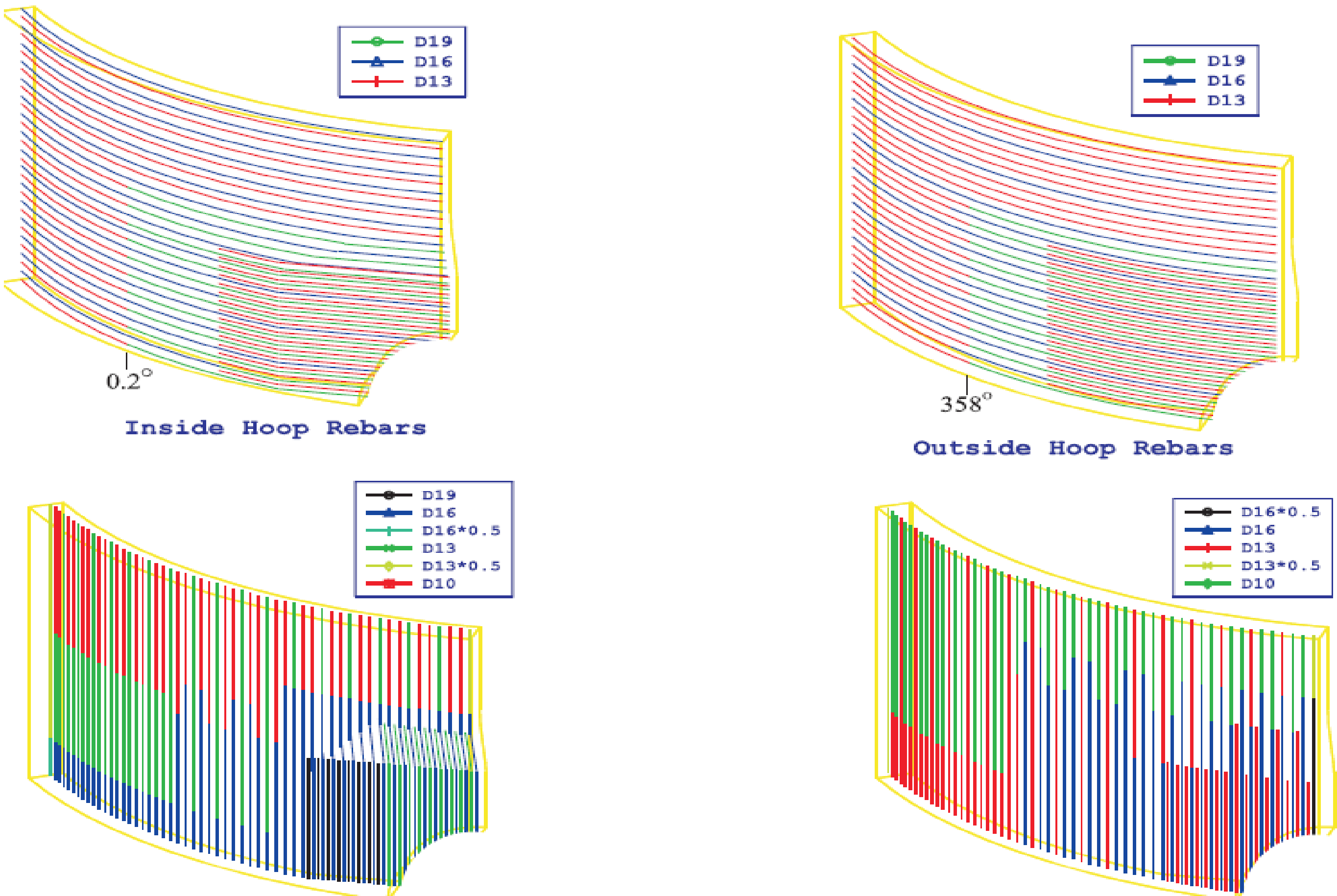

(Important to Simulating Strain Concentrations)

MOFFATT & NICHOL

Sandia National Laboratories

Model Geometry and Initial Conditions

- Concrete modeled with 8-node 3D solid elements, rebar modeled with embedded subelements, tendons with two-node truss elements, and liner with 4-node shell elements
- Losses handled by initial conditions applied to tendons and by FE Model's representation of angular friction
- Every tendon was modeled

Prestressing Tendon Geometry for Model 2

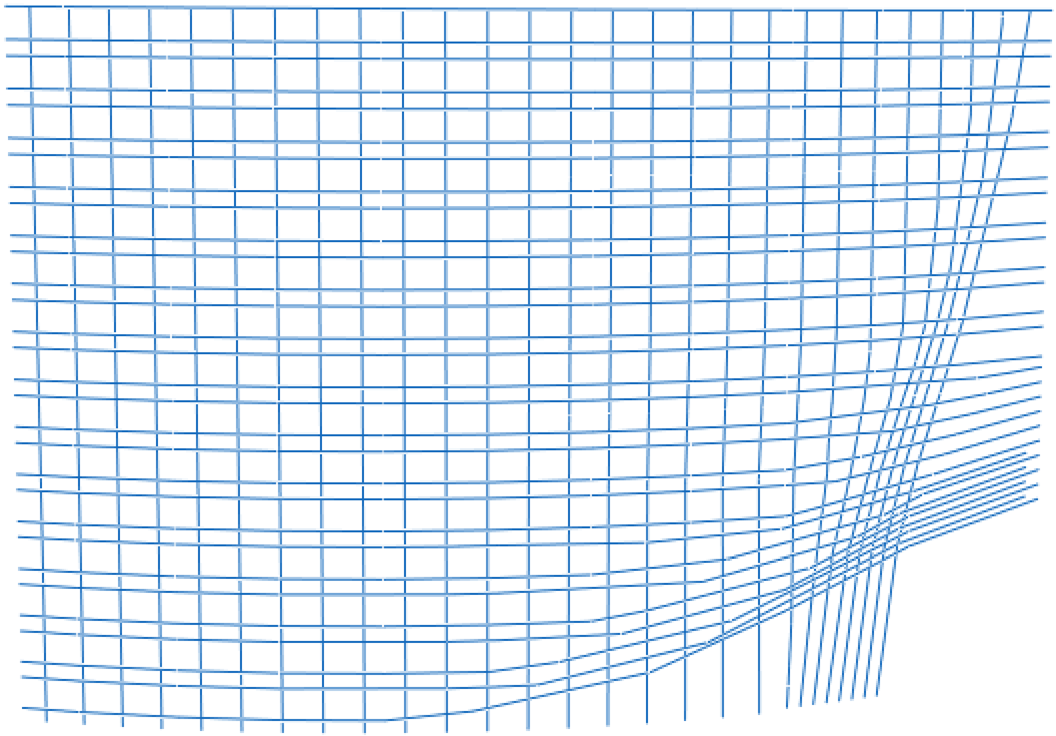

MOFFATT & NICHOL

Sandia National Laboratories

Model Geometry and Initial Conditions

- With methodology in Model 1, contact condition requires nodes of tendon and nodes of concrete be coincident
- Making concrete mesh compatible with tendon mesh is extremely difficult and time consuming
- Strategy developed to facilitate modeling of tendon-concrete interaction – embedded shell elements created, surrounding each tendon (analogous to “sheaths” or “ducts”)
- Elements fully embedded into concrete, while allowing contact surface to follow 3d geometry and effectively model actual conditions

Sheath Elements Along Tendon with Jacking Elements

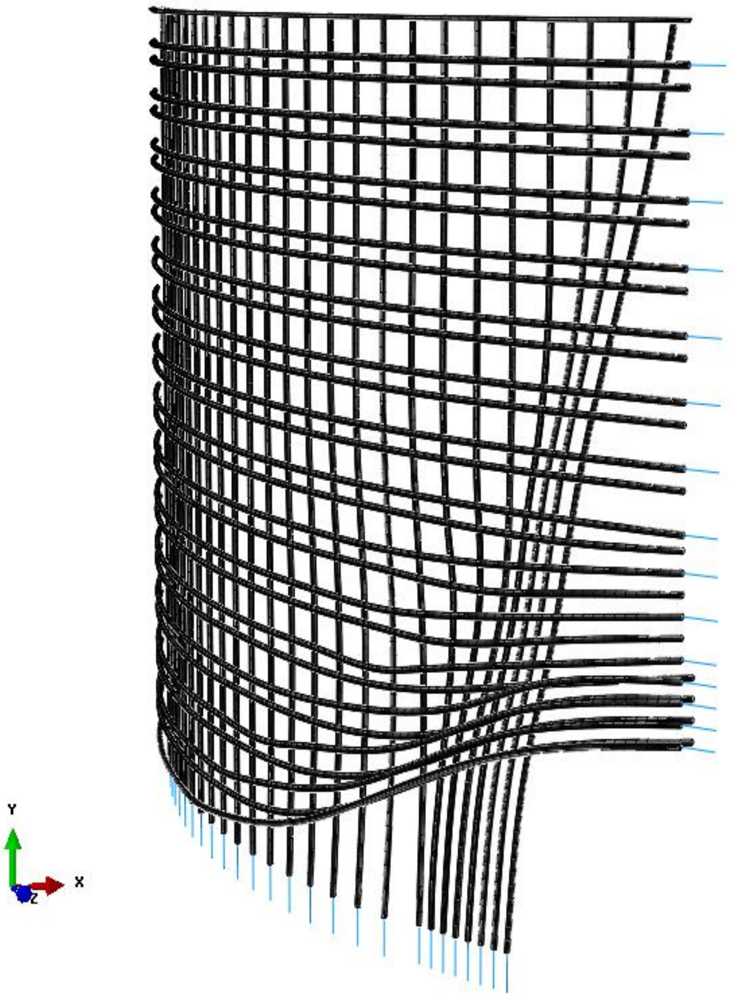

MOFFATT & NICHOL

Sandia National Laboratories

Tendons Inside Duct

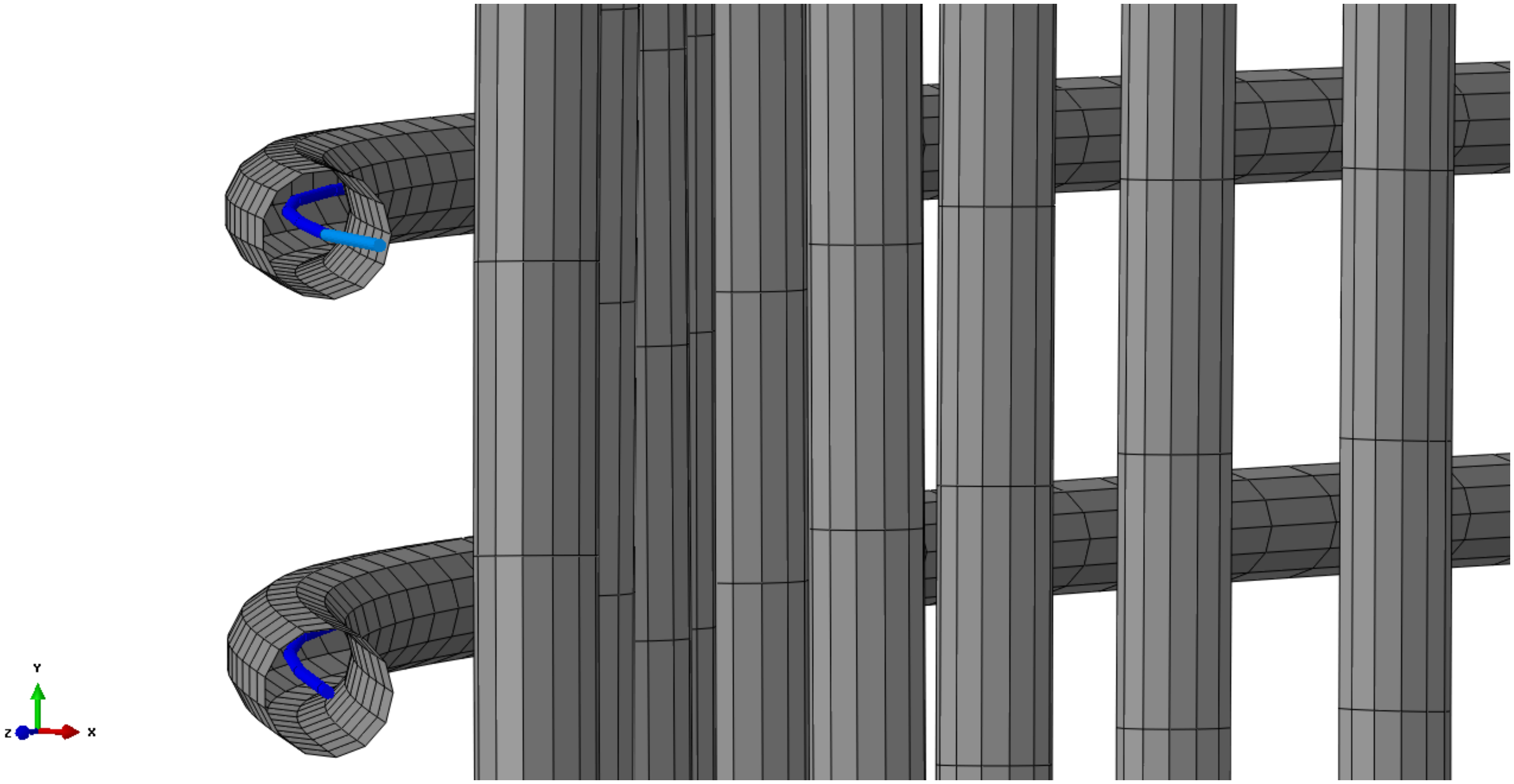

MOFFATT & NICHOL

Sandia National Laboratories

Model Geometry and Initial Conditions

- Ends of tendons have a 'jacking element' protruding from the edge of concrete mesh
- For Model 2, jacking 'element' assigned only on one side of each tendon, the side closest to the buttress the tendon is jacked from
- Other end of each tendon tied to concrete face
- This geometry difficult to set up, some unavoidable edge effects which influence the tendon stresses and strains of the end element, the tendon stress and strain distributions interior to these end elements appear to be reasonable

Model Overview

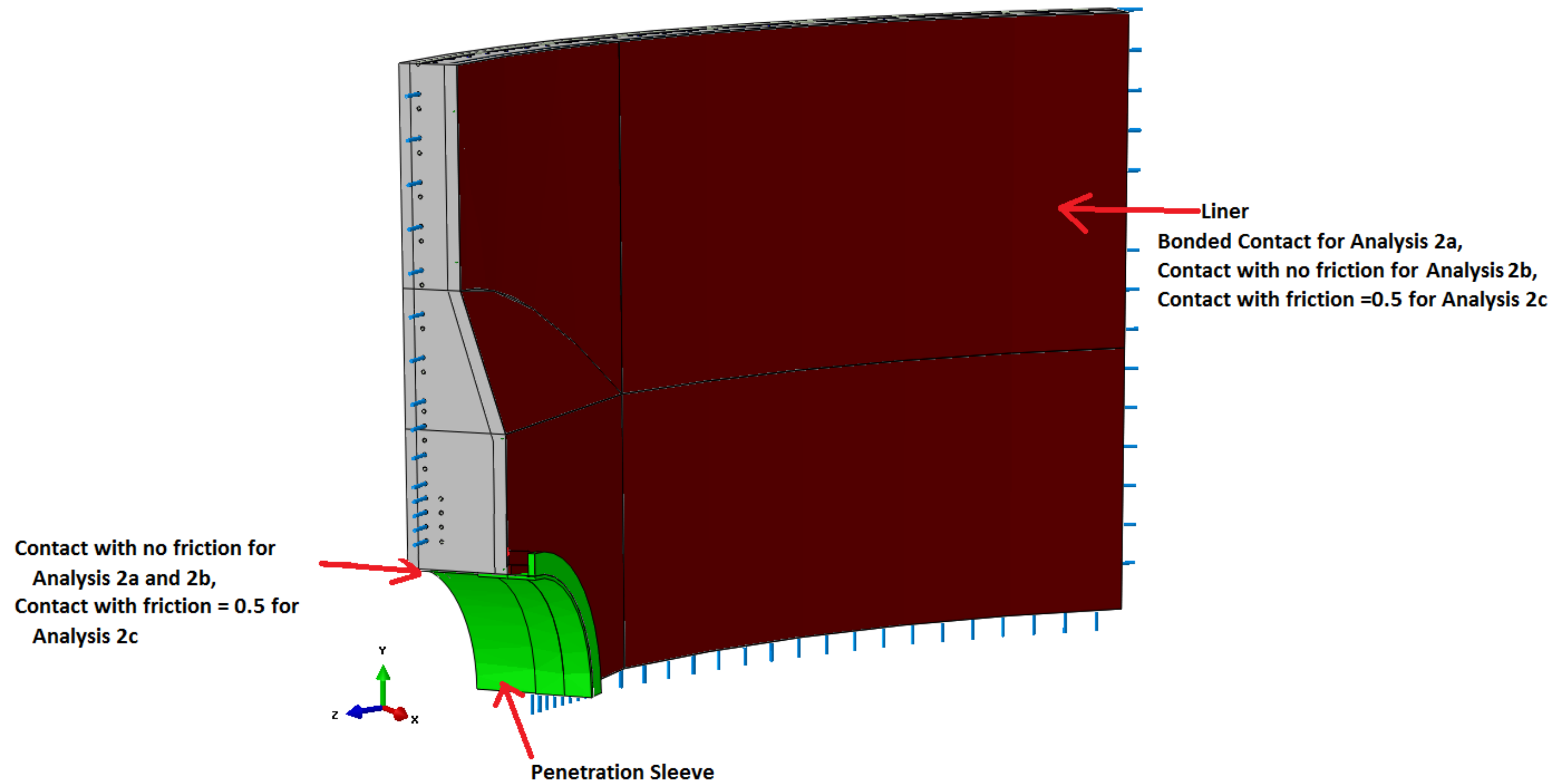

Tendon Sheaths with Jacking Elements Shown

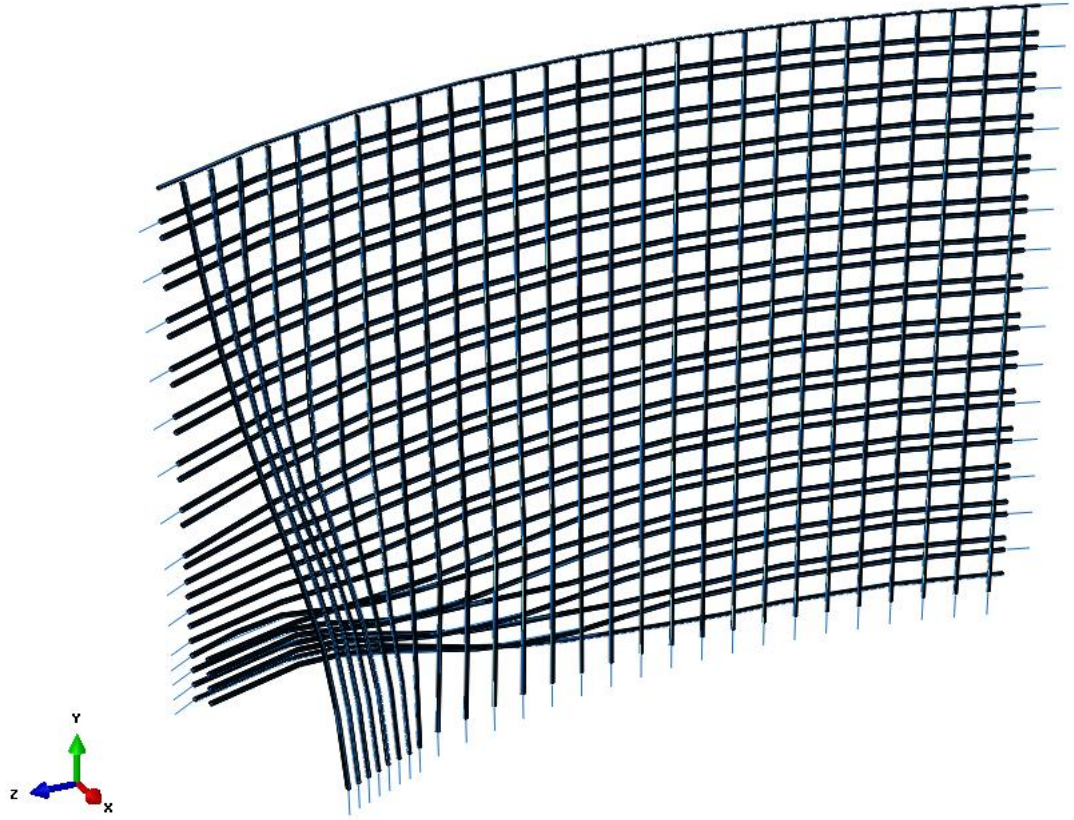

MOFFATT & NICHOL

Sandia National Laboratories

Concrete Mesh

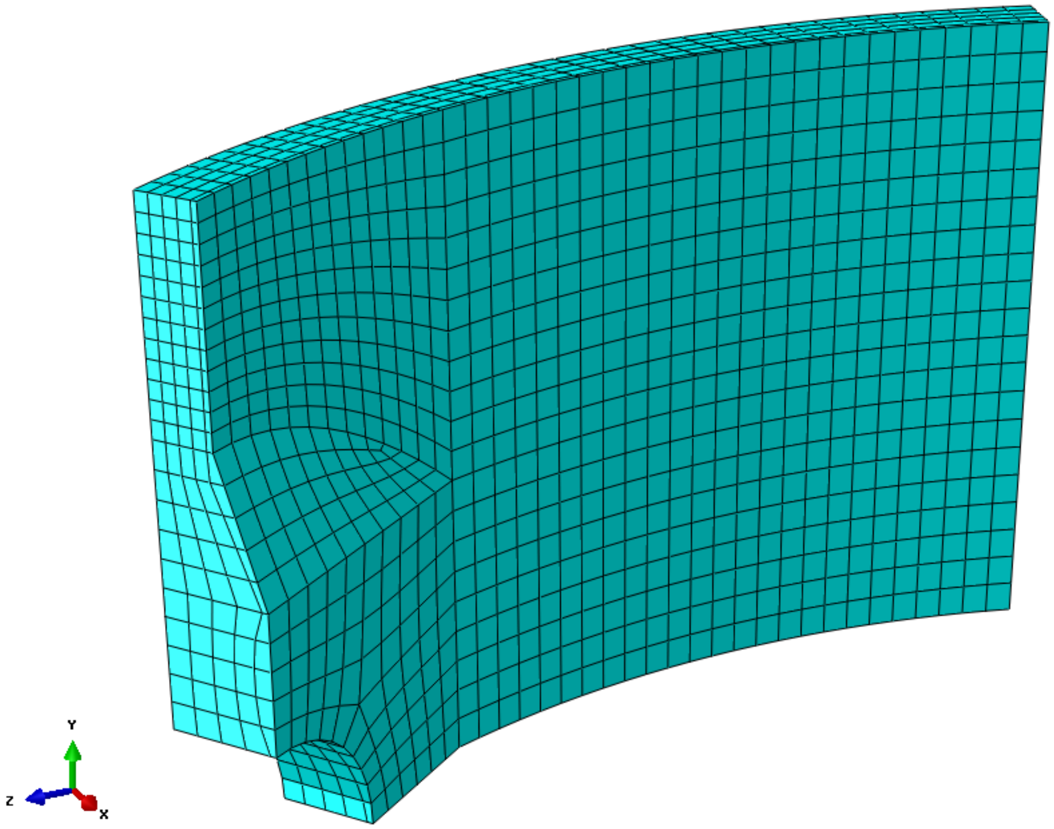

Steel Liner and Penetration Pipe Mesh

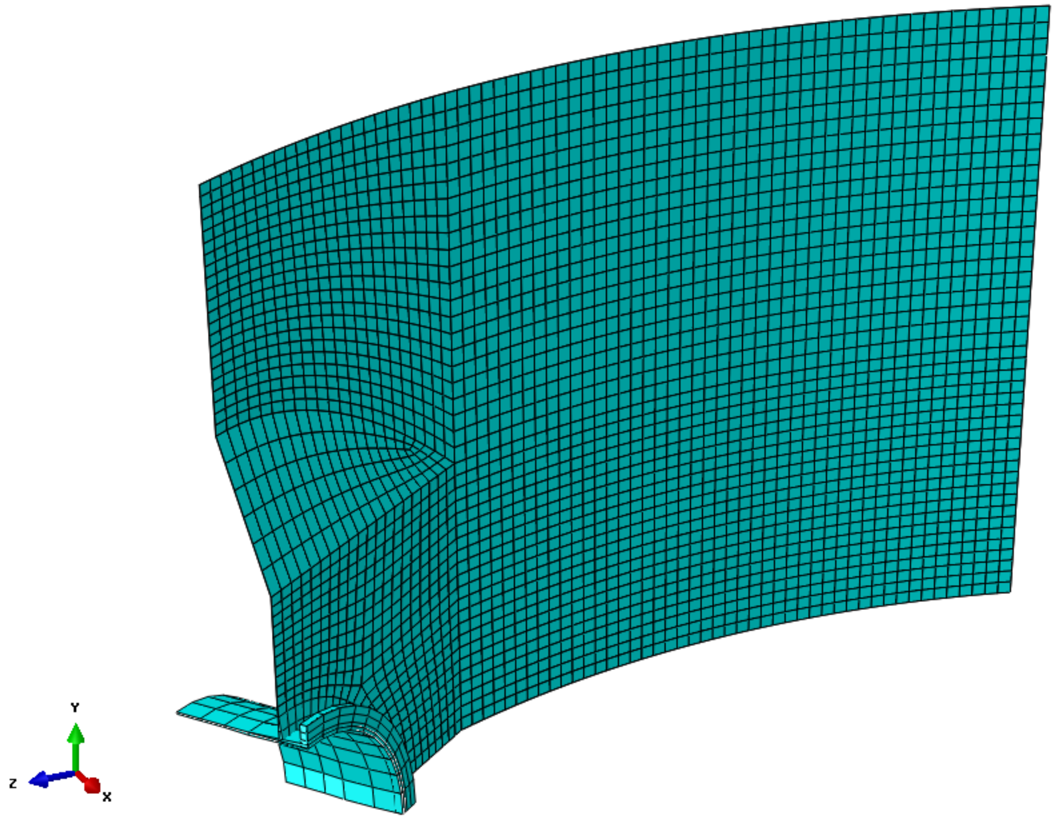

MOFFATT & NICHOL
Sandia National Laboratories

Vertical and Horizontal Liner Anchors

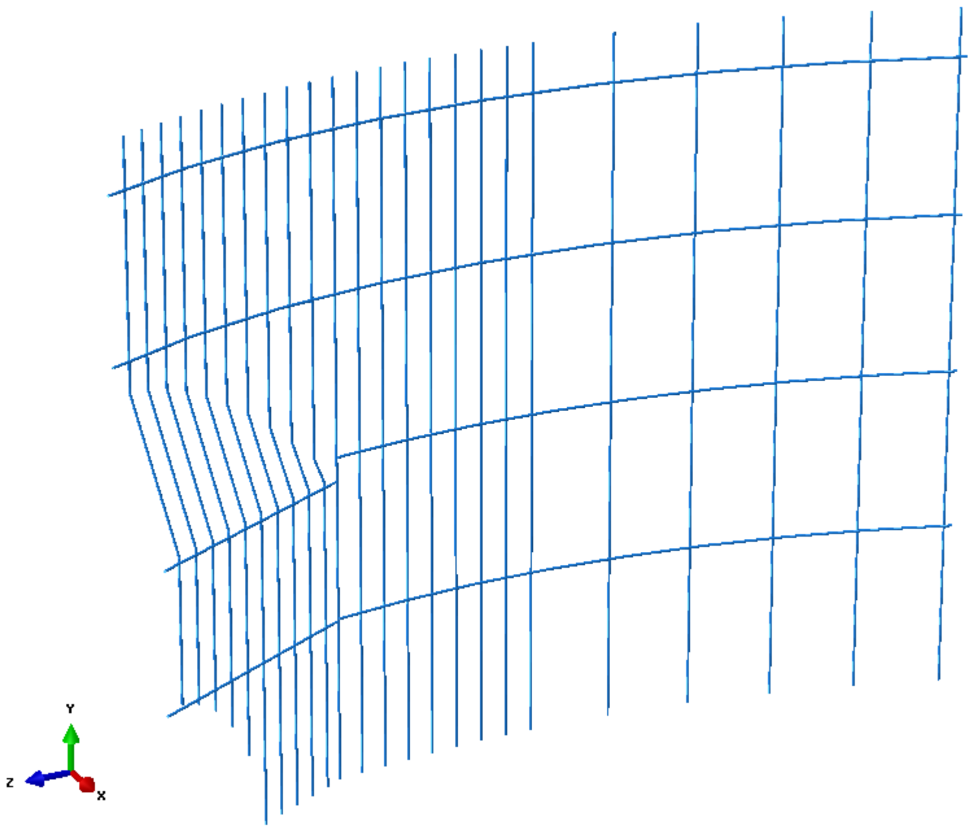

MOFFATT & NICHOL

Sandia National Laboratories

Liner Tear Locations

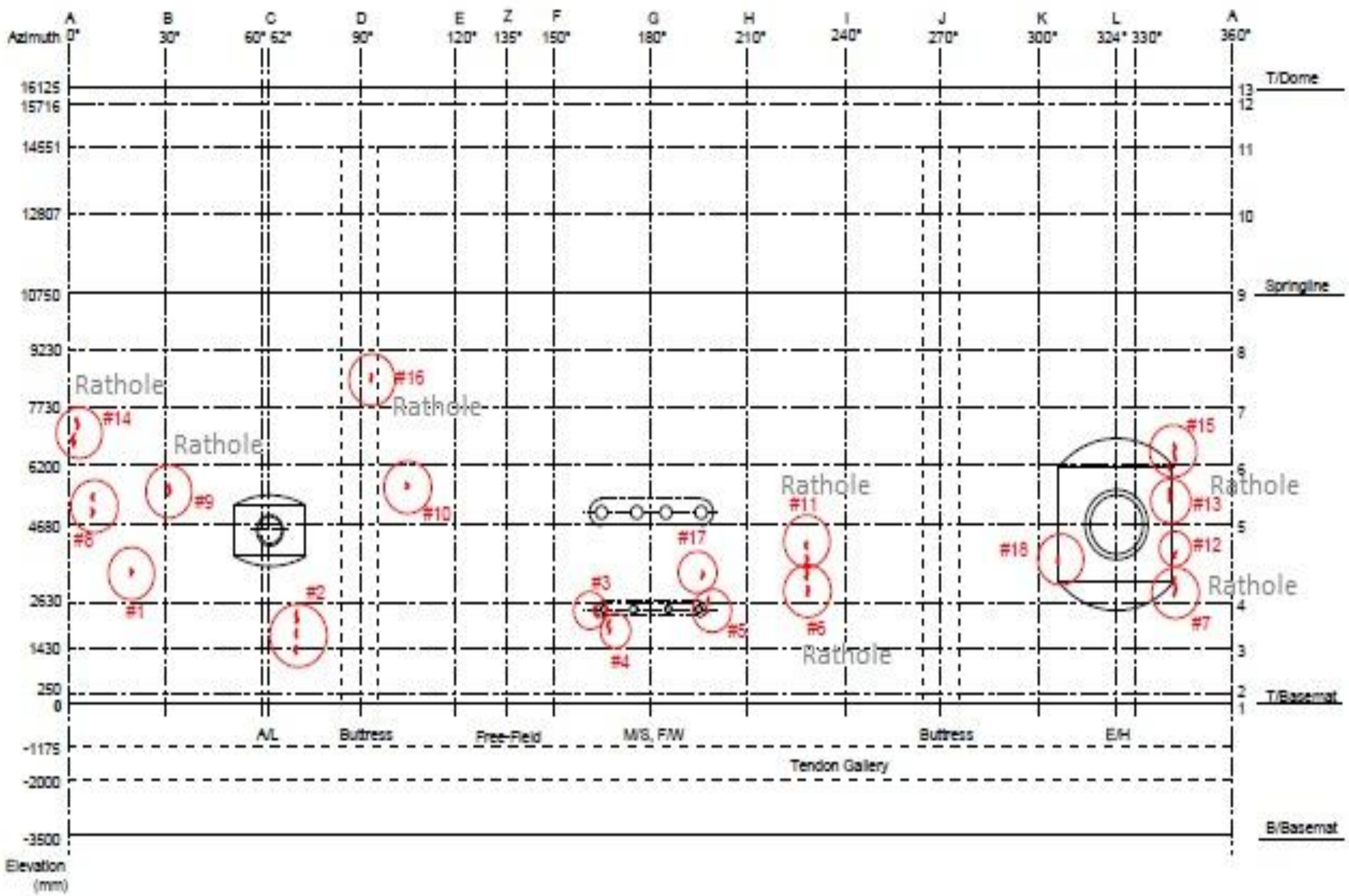

MOFFATT & NICHOL

Sandia National Laboratories

Key Locations for Reporting Liner Strain Selected for Model 2 Exercise

Objectives:

1. To choose a relatively long gage length over which to report strain in order to eliminate differences between analysts due to mesh size
2. To focus on key aspects of liner-concrete interaction
3. Establish a framework for a fracture-mechanics based liner failure prediction

- Locations are numbered 1 through 10, boundaries are defined by liner anchors
- At large anchor spacing, gage length is 450.45mm
- Locations 5 and 10 straddle two anchor spaces, for a gage length equal to 300.30mm

Liner (E/H) View Showing Strain Reports (cut from Page A-28 of NUREG/CR-6810)

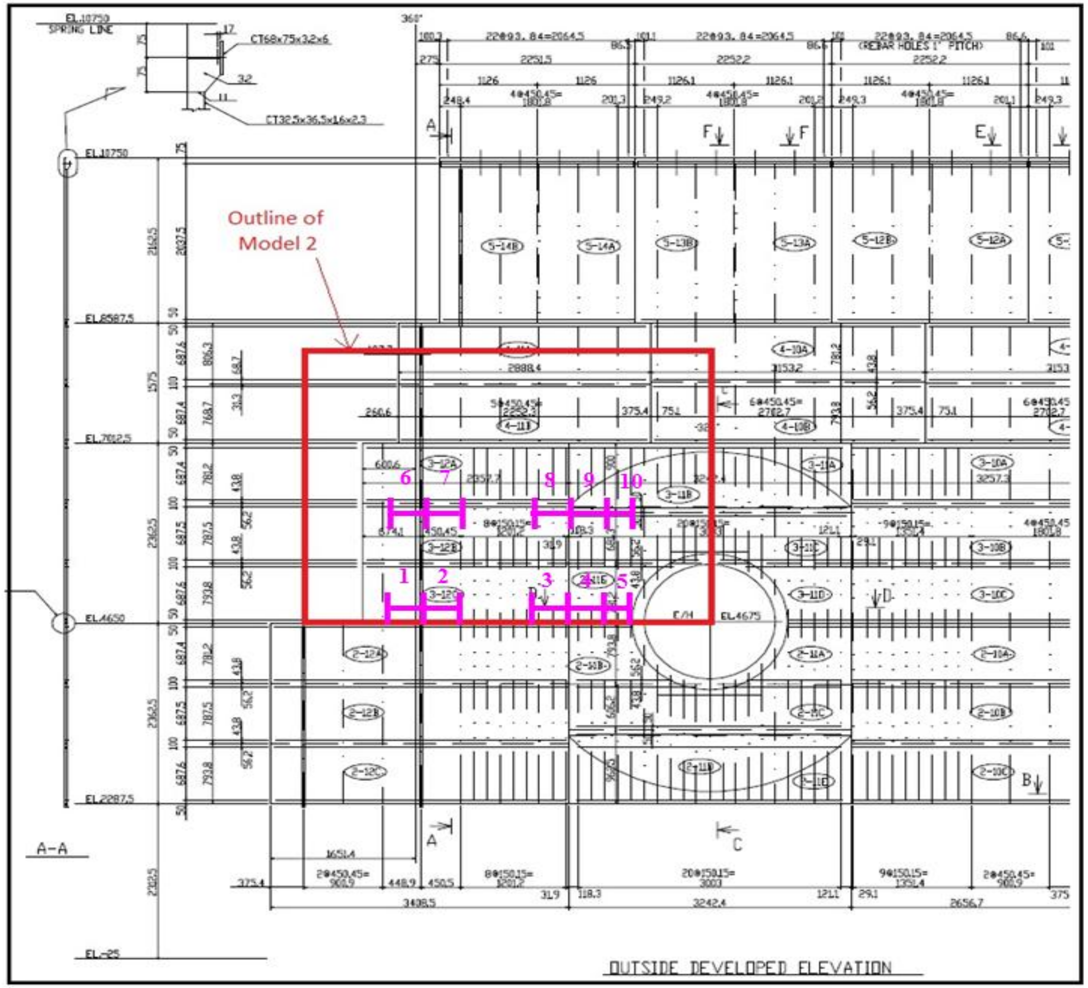

MOFFATT & NICHOL

Sandia National Laboratories

Information About Tendon Friction and Seating Losses

- Some tendons being jacked from 270° have additional losses as they sweep around the Equipment Hatch before reaching the region of Model 2
- These tendons have same anchor stress after losses as the free-field hoop tendons

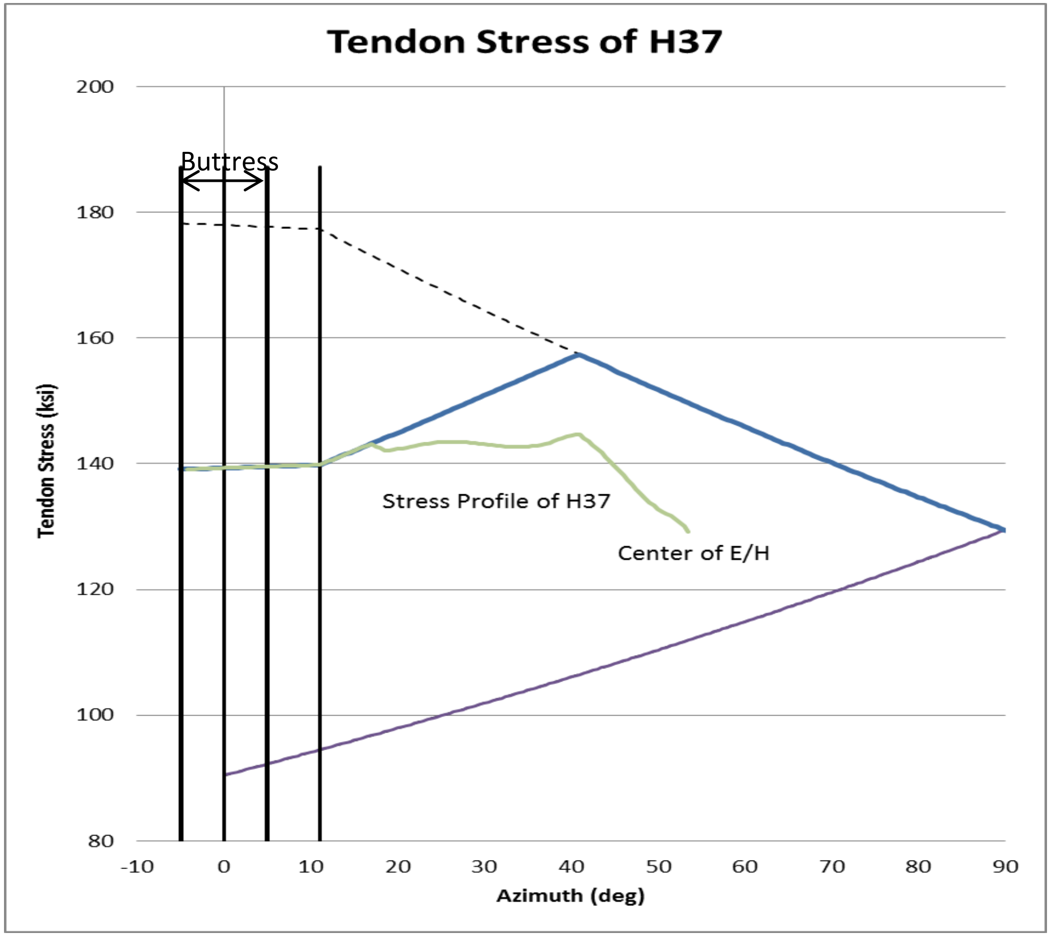

Tendon Stress Applied to Jacking End of Model 2

Jacked from 270°	
Tendon	Stress (MPa)
H37	890
H39	885
H41	873
H43	901
H45	962
H47	1,006
H49	1,015
H51	1,030
H53	1,030
H55	1,030
H57	1,030
H59	1,030
H61	1,030
H63	1,030
H65	1,030

Jacked from 90°	
Tendon	Stress (MPa)
H38	959
H40	959
H42	959
H44	959
H46	959
H48	959
H50	959
H52	959
H54	959
H56	959
H58	959
H60	959
H62	959
H64	959
H66	959

Jacked from Basemat	
Tendon	Stress (MPa)
V59	1,130
V60	1,130
V61	1,130
V62	1,130
V63	1,130
V64	1,130
V65	1,130
V66	1,130
V67	1,130
V68	1,130
V69	1,130
V70	1,130
V71	1,130
V72	1,117
V73	1,102
V74	1,090
V75	1,076
V76	1,065
V77	1,054
V78	1,057
V79	968
V80	978
V81	968
V82	968
V83	948
V84	950
V85	943

- **For Model 2c, estimate for stiffness and strength of liner is needed to complete the simulation**
- **Detailed local models for vertical and horizontal anchors created to obtain force-versus deflection curves**
- **Used to determine stiffness of springs connecting the steel liner to the anchors**
- **For anchor to concrete interaction, a friction coefficient of 0.5 was used**
- **Liner has fully yielded at the anchor, and the concrete is crushing**
- **This data converted to a bilinear curve**
- **Results of the local models were applied in the direction perpendicular to the direction of the anchor**

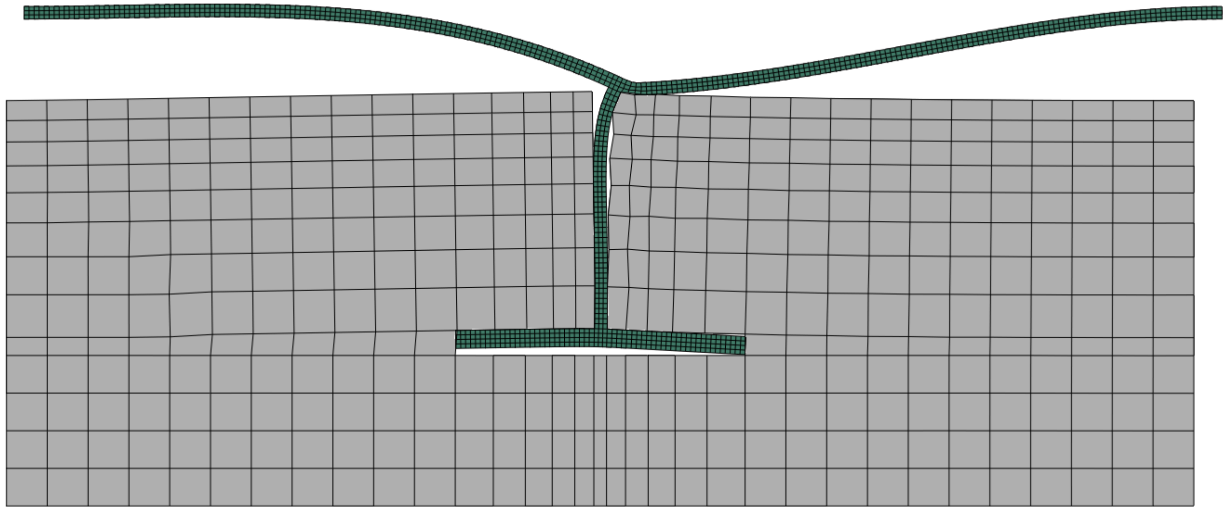

Vertical Liner Anchor Local Model at 10x deformed shape

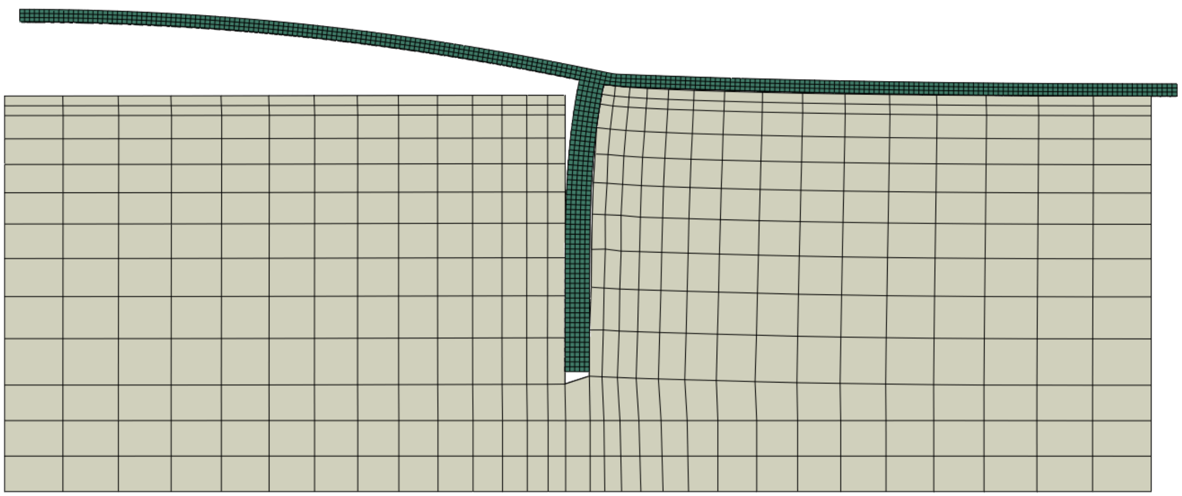

Horizontal Liner Anchor Local Model at 10x deformed shape

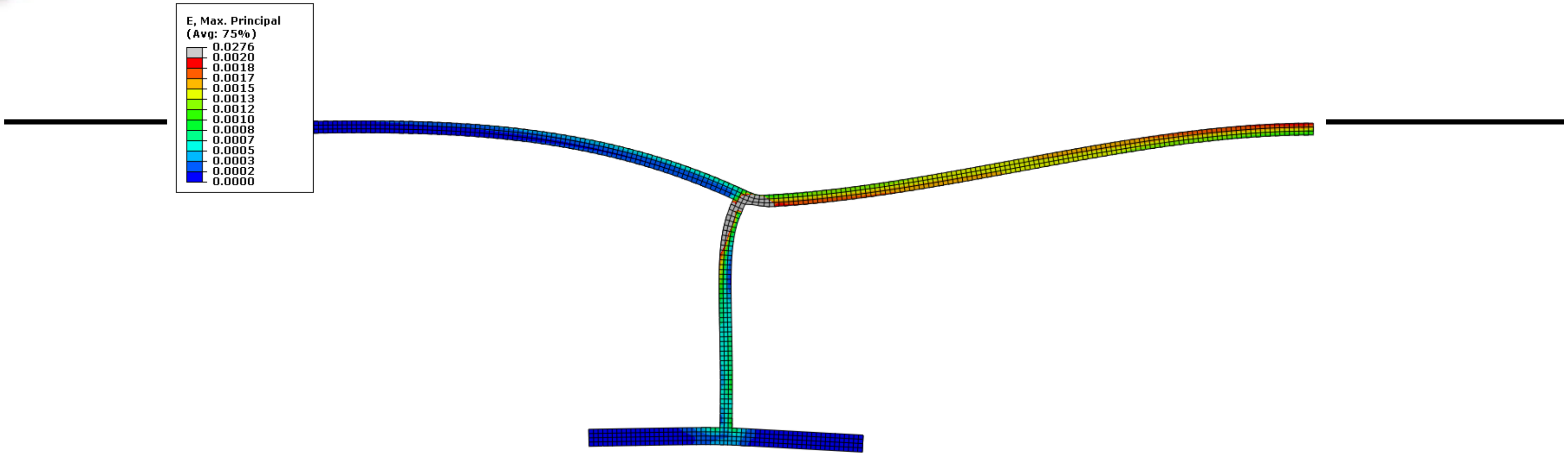

Max Principal Strain in Liner and Vertical Anchor

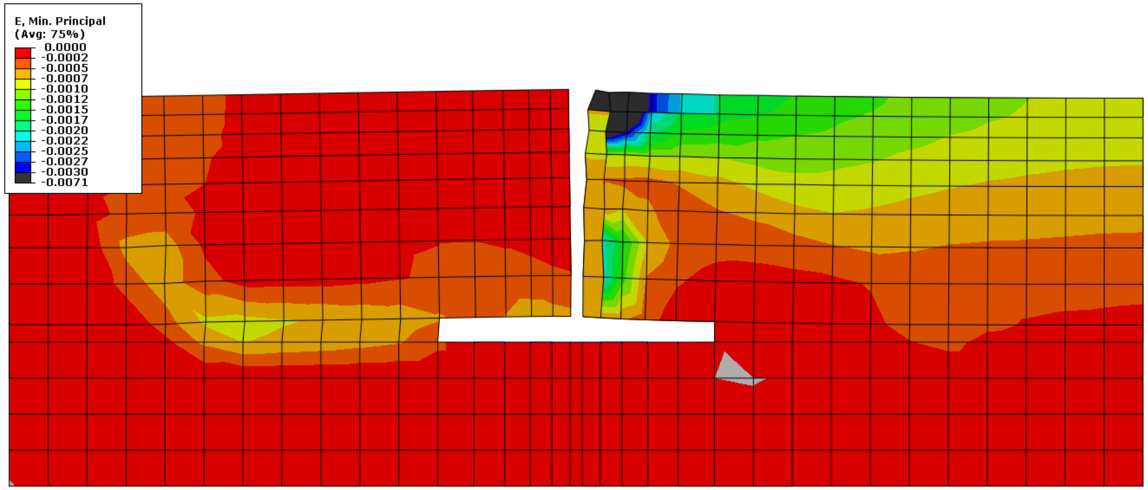

Min Principal Strain in Liner and Vertical Anchor

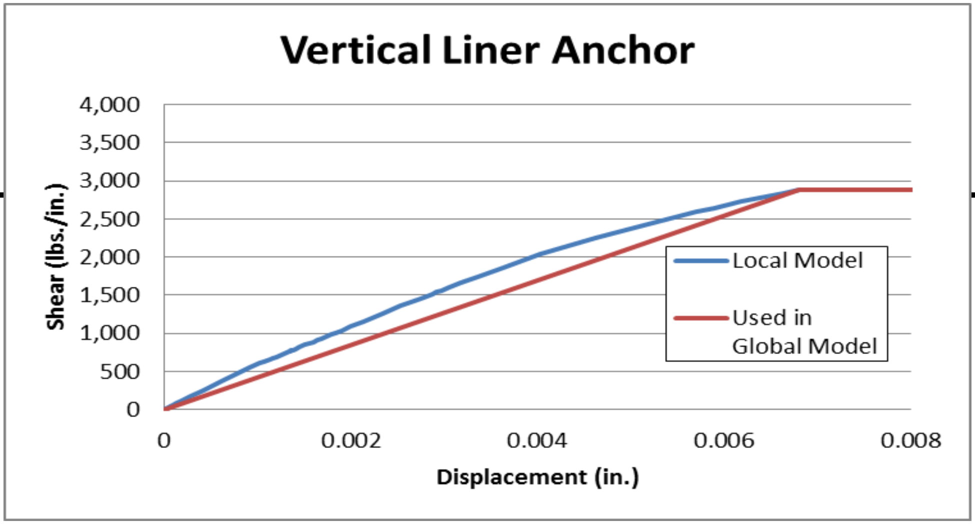

Force-Deflection Curve for Vertical Liner Anchor

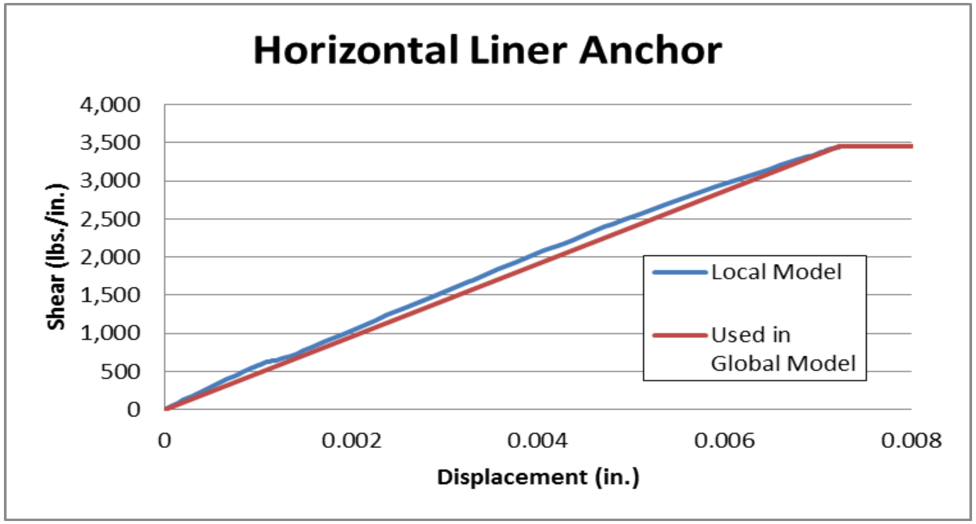

Force-Deflection Curve for Horizontal Liner Anchor

Failure Criteria

- **For Model 2, tendon criteria remains at 3.8% strain as for Model 1**
- **But Model 2 is also focused on liner tear and leakage**

Biaxial-Stress Liner Failure Criteria

$$\mu = 2^{(1-\mathrm{TF})}$$

where: μ is the ductility (reduction) ratio
TF is the Davis Triaxiality factor

$$\mathrm{TF} = \frac{\sqrt{2}\,(\sigma_1 + \sigma_2 + \sigma_3)}{\left[(\sigma_1 - \sigma_2)^2 + (\sigma_2 - \sigma_3)^2 + (\sigma_3 - \sigma_1)^2\right]^{1/2}}$$

But when the third principal stress is zero or nearly zero, as in the case of the TBT shell plates,

$$\mathrm{TF} = \frac{(\sigma_1 + \sigma_2)}{(\sigma_1^2 - \sigma_1\sigma_2 + \sigma_2^2)^{1/2}}$$

For instance when σ_1 and σ_2, TF = 2 and the ductility ratio is 0.5

Biaxial-Stress Liner Failure Criteria

- Many containment analysts have concluded there is extensive judgment involved in its application
- Strains predicted by FE models can be highly dependent on the level of detail (and mesh refinement)
- The existence of flaws in the material (especially at weld seams) mean that tears might occur with strains significantly lower than the absolute ductility of the material

Analysis Results

- **Model 2 was analyzed with three sets of liner-concrete interaction assumptions**

  2a) Liner assumed bonded (no-slip) to concrete

  2b) Liner only connected to concrete at anchors, free-slip in between

  2c) Best estimate connection and consideration of friction

Required Output/Results for Model 2

1. Description of modeling assumptions and phenomenological models
2. Description of liner failure criteria used
3. Pressure milestones. Applied pressure:
   i) Where and when concrete hoop cracking occurs
   ii) First tendon reaches 1% strain
4. Deformed shape and liner strain distribution at P=0 (prestress applied); $1xP_d$; $1.5P_d$; $2P_d$; $2.5P_d$; $3P_d$; $3.3P_d$; $3.4P_d$; Ultimate pressure
5. Liner strain magnitudes (hoop direction) at locations indicated in Figure
6. Ovalization: Change in diameter of hatch and adjacent concrete, in hoop direction, versus pressure
7. Ovalization: Change in diameter hatch and adjacent concrete, in Meridional direction, versus pressure

Results by Pressure Milestones

Milestone	Pressure (MPa)	x Pd
Zero Concrete Hoop Stress (at 0° azimuth)	0.534	1.36
Concrete Hoop Cracking Occurs (at 0° azimuth)	0.585	1.49
Tendon A and B Reach approx.1% Strain (at 0° azimuth)	1.362	3.47

MOFFATT & NICHOL

Sandia National Laboratories

Results and Observations

- The results for 2b) and 2c) are similar, so no separate plots
- Significant differences begin occurring at $3.0xP_d$
- The yield strain for the liner is 0.0018
- Pockets of yielding begin to occur at $2.5xP_d$, and become widespread by $3.0xP_d$
- First yielding occurs in area adjacent to liner thickness transition near hatch and in larger areas between 0-degree and 18-degrees azimuth. Note that near 0-degrees is where transition occurs in hoop rebar area density

Results and Observations

- Elevated strain zones are somewhat more prevalent in Model 2b and 2c than in Model 2a
- By 3.3xP_d, many elevated liner strain zones are reaching 0.01, and by 3.7xP_d, 0.014 to 0.017 or nearly 2% strain
- Agree reasonably well with observed behaviors from the 1:4 Scale Model Test
- Mesh size of 2”-3” for modeling the liner
- With this mesh-size, we would not anticipate predicting as large of localized liner strains as may occur at an individual strain gage

Results and Observations

- Ovalization of the penetration sleeve, and resulting separation between pipe and concrete
- Found differences in diameters (both horizontal and vertical) between the pipe and concrete are not uniform through the thickness
- We plotted the separation gap between the penetration surface and the concrete surface
- No significant separation until approximately $2.5P_d$, but then separations of 0.03 inch, 0.08 inch 0.12 inch, 0.14 inch, and 0.16 inch for $2.5P_d$, $3.0P_d$, $3.3P_d$, $3.4P_d$, and $3.47P_d$, respectively
- Model 2a showed more separation than Model 2b and 2c
- Maximum separation occurs at 2 o'clock position of E/H

Min Principal Stress (psi) in Concrete Under Prestress Only

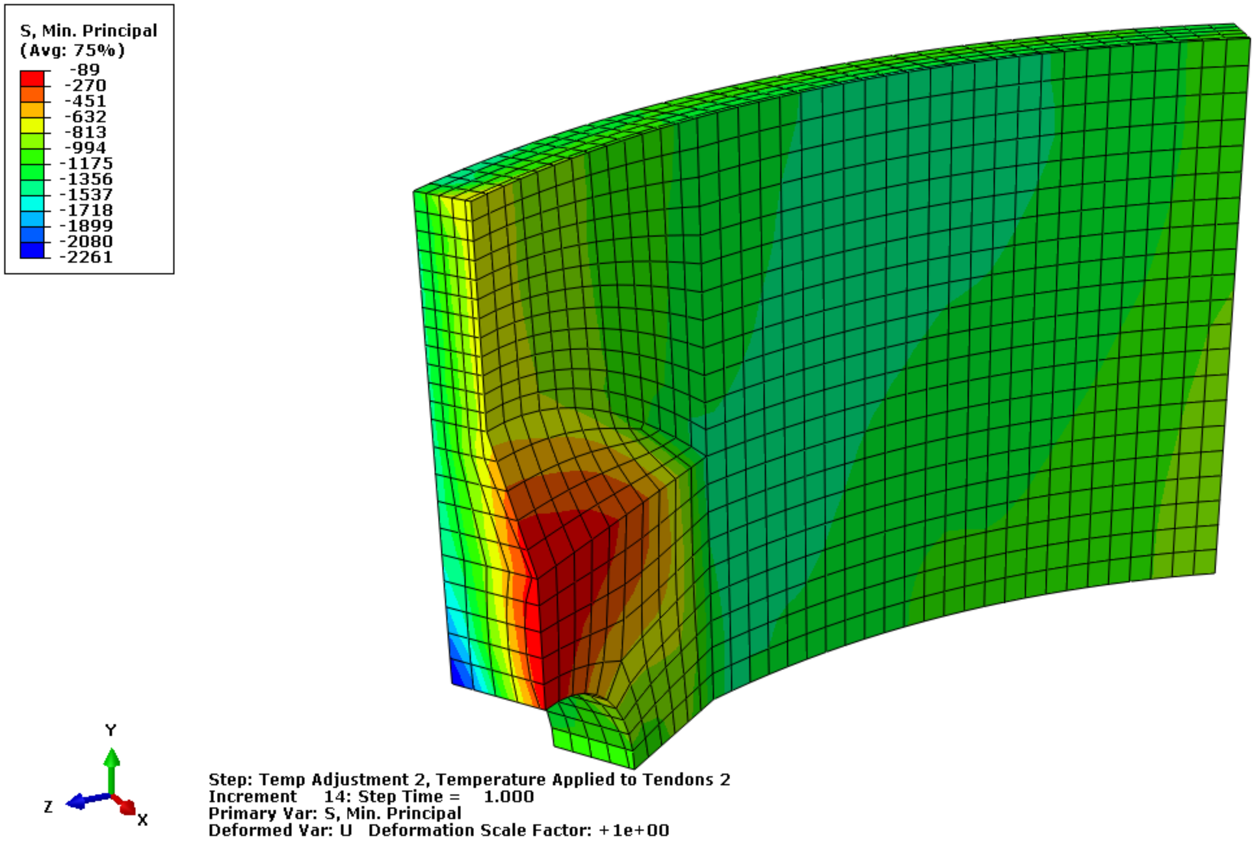

MOFFATT & NICHOL

Sandia National Laboratories

Tendon Stresses (psi) After Prestress Only

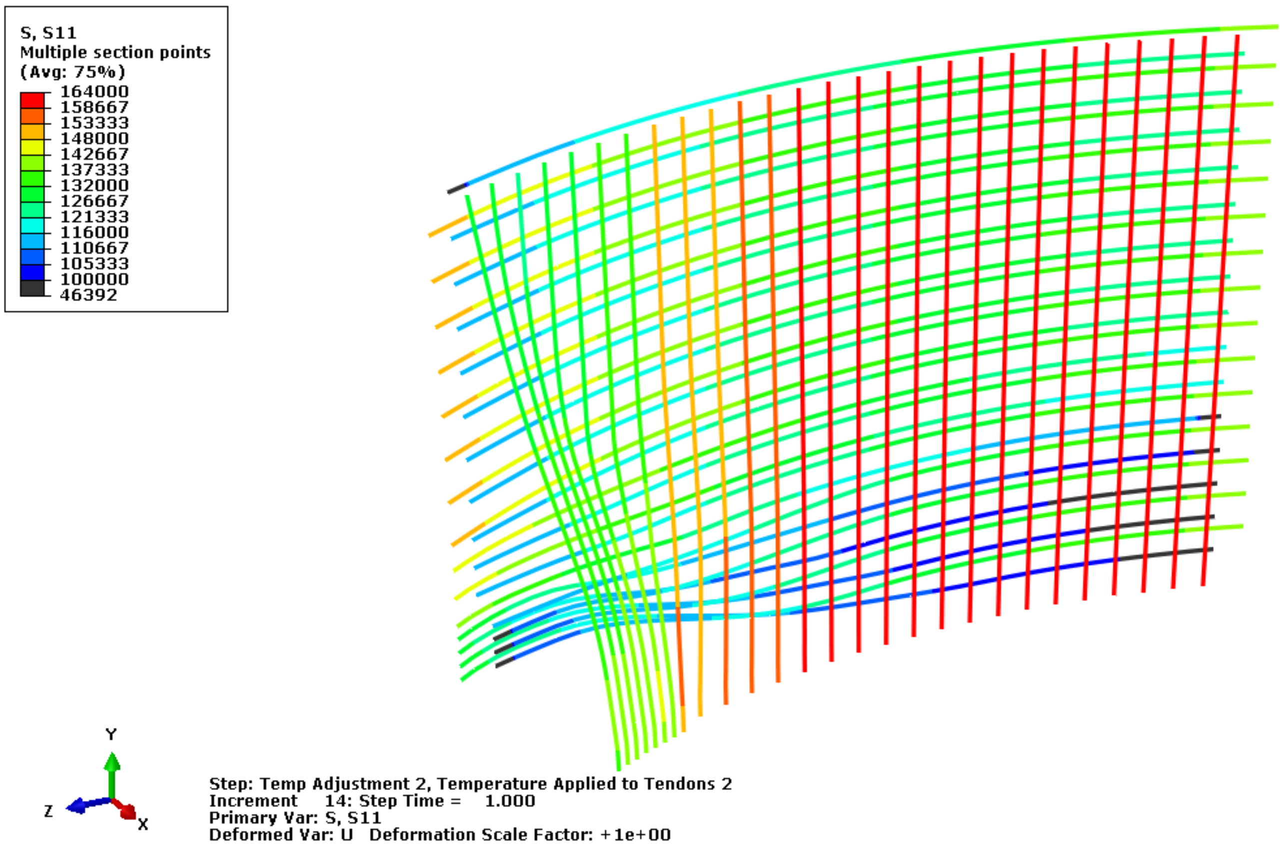

Tendon Stresses (psi) with 3.3xP_d

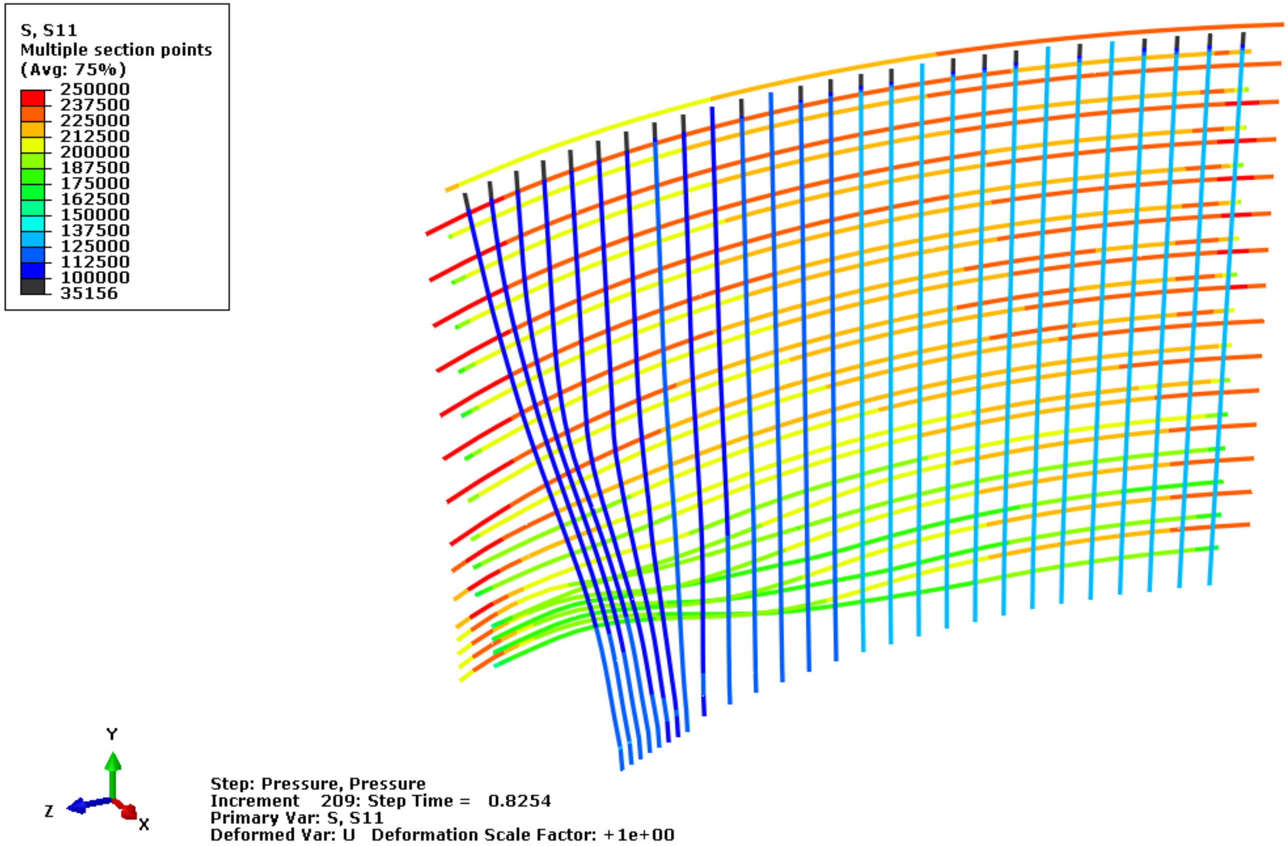

MOFFATT & NICHOL

Sandia National Laboratories

Tendon Stresses (psi) with 3.47xP_d

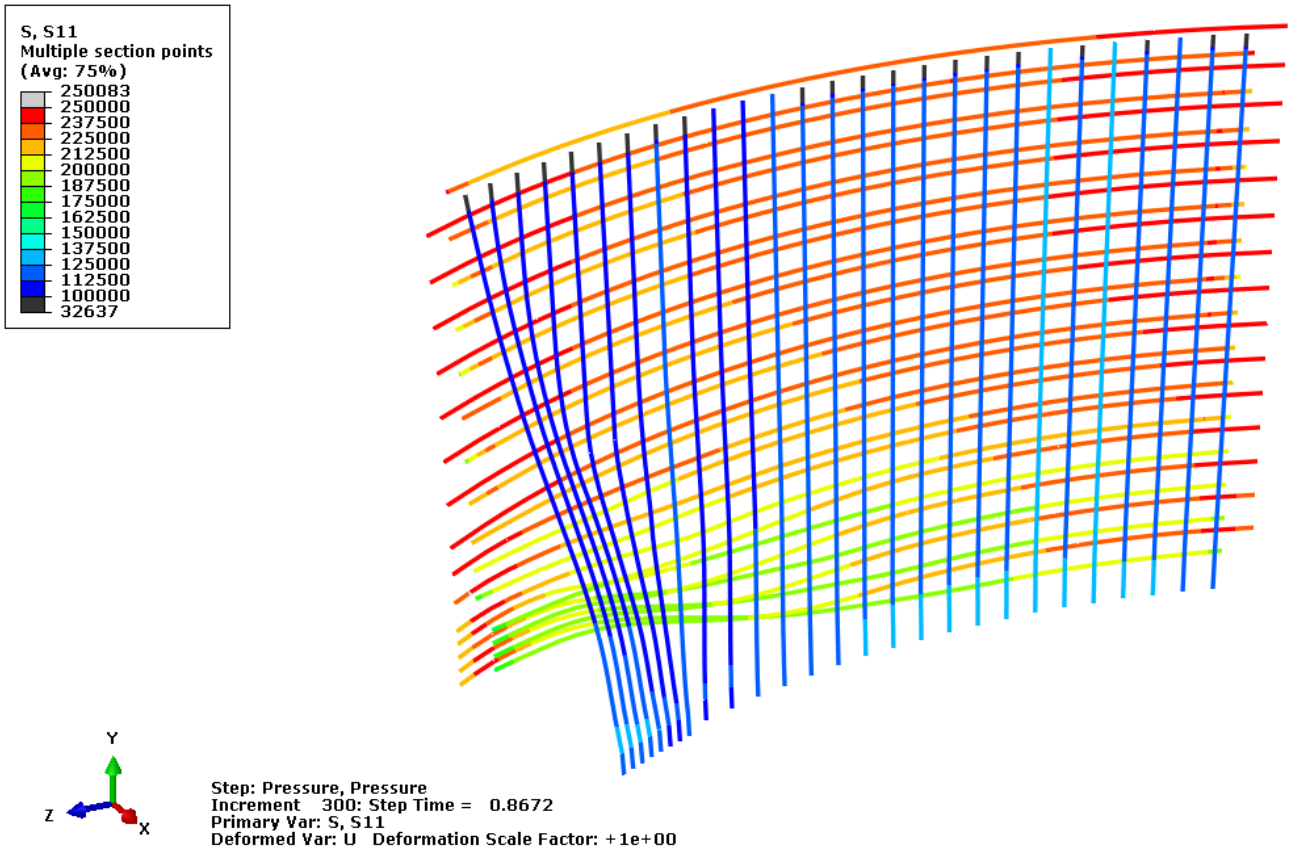

MOFFATT & NICHOL

Sandia National Laboratories

Tendon Strain with 3.47xP_d

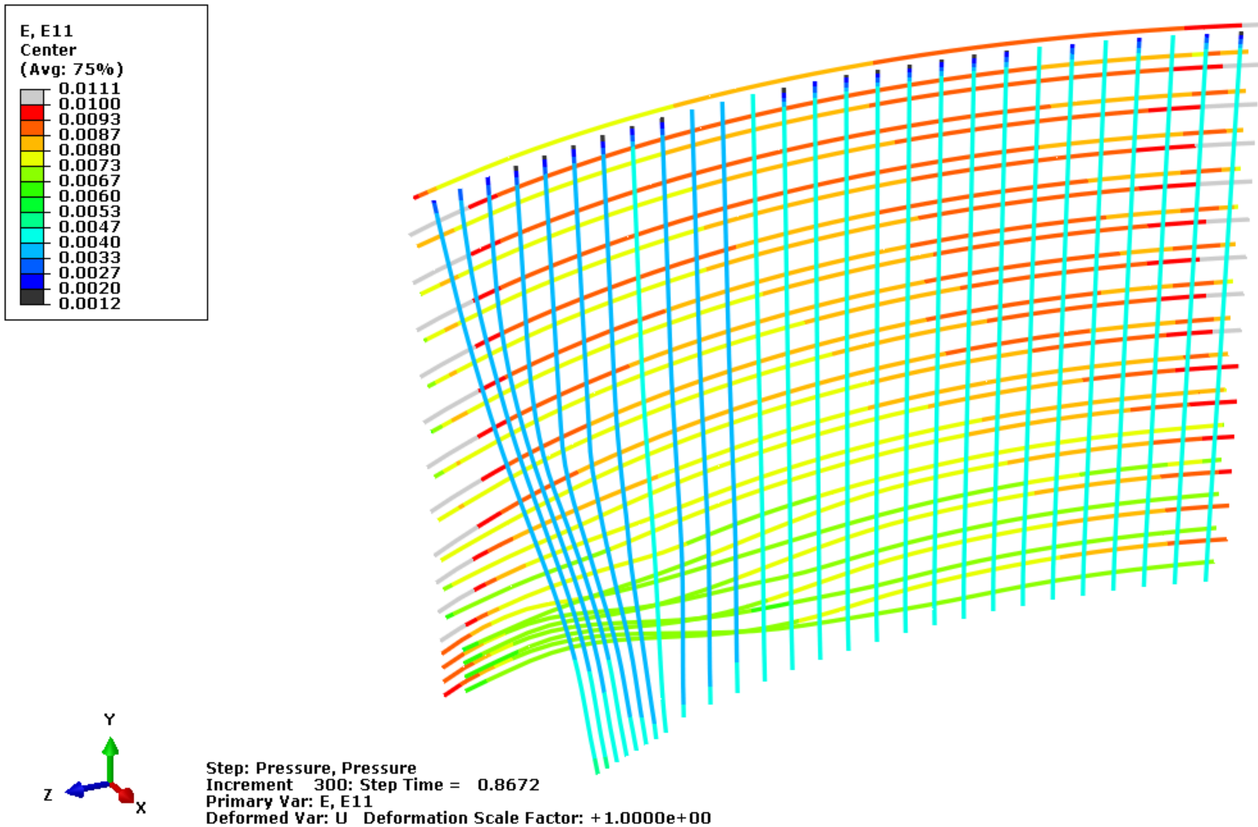

Liner Max Principal Strains at 2.0xP_d

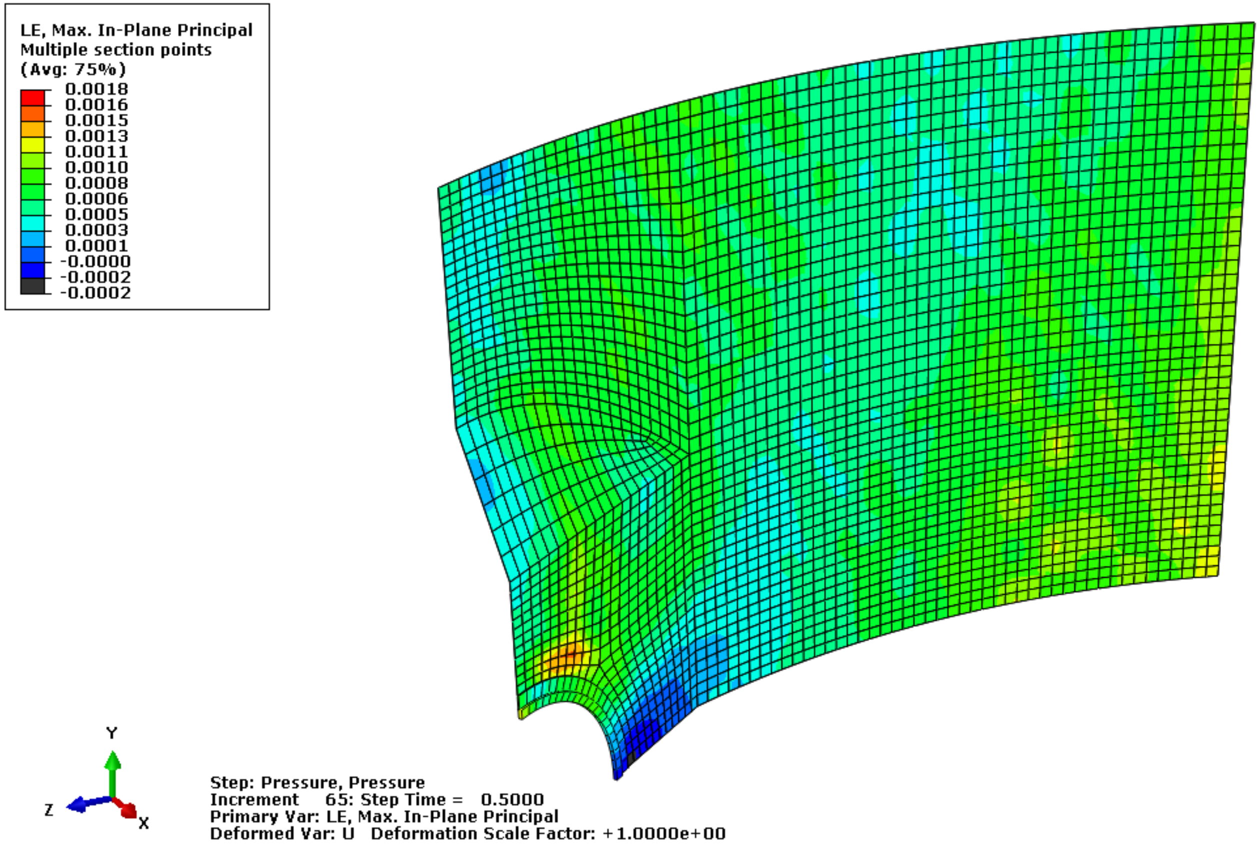

MOFFATT & NICHOL

Sandia National Laboratories

Liner Max Principal Strains at $3.0xP_d$ for Model 2a

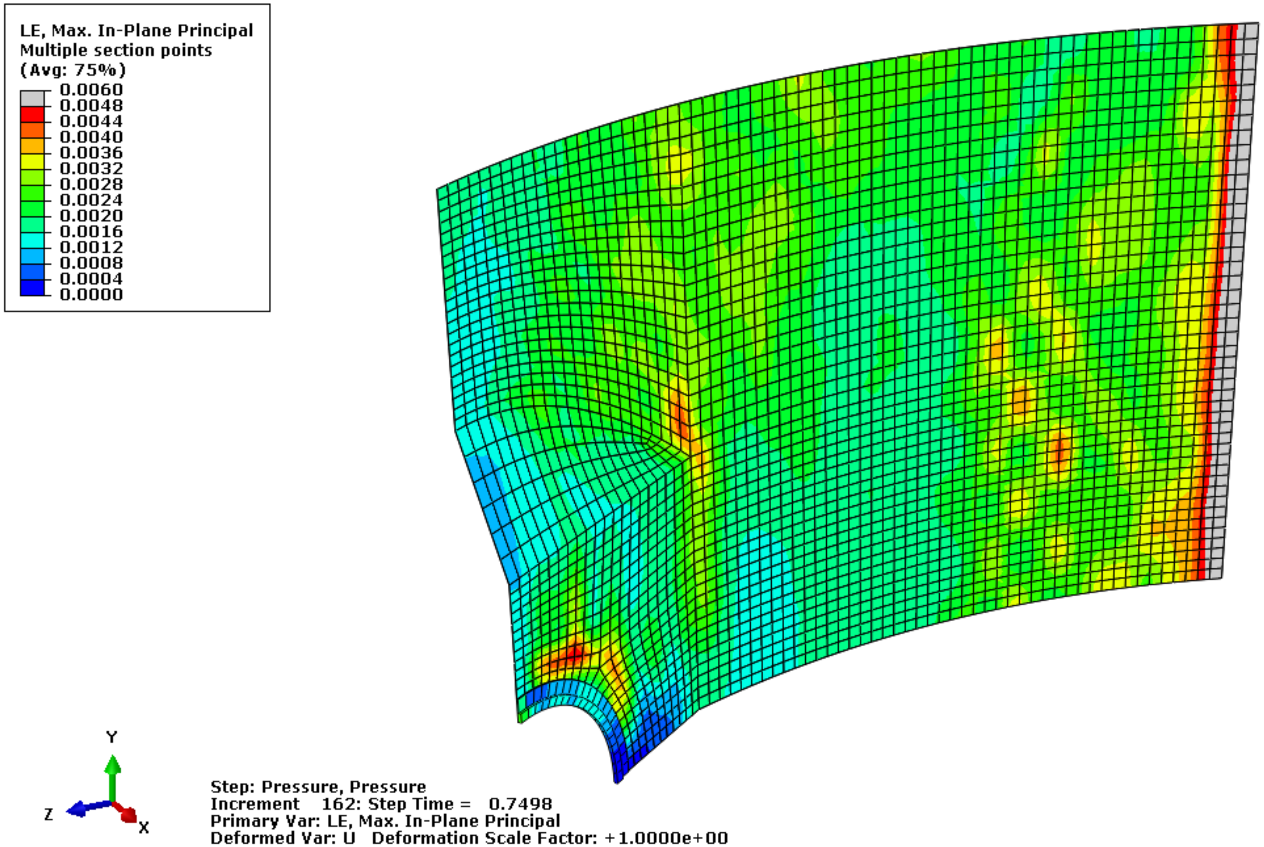

(note change in contour limits)

MOFFATT & NICHOL

Sandia National Laboratories

Liner Max Principal Strains at 3.3xP$_d$ for Model 2a

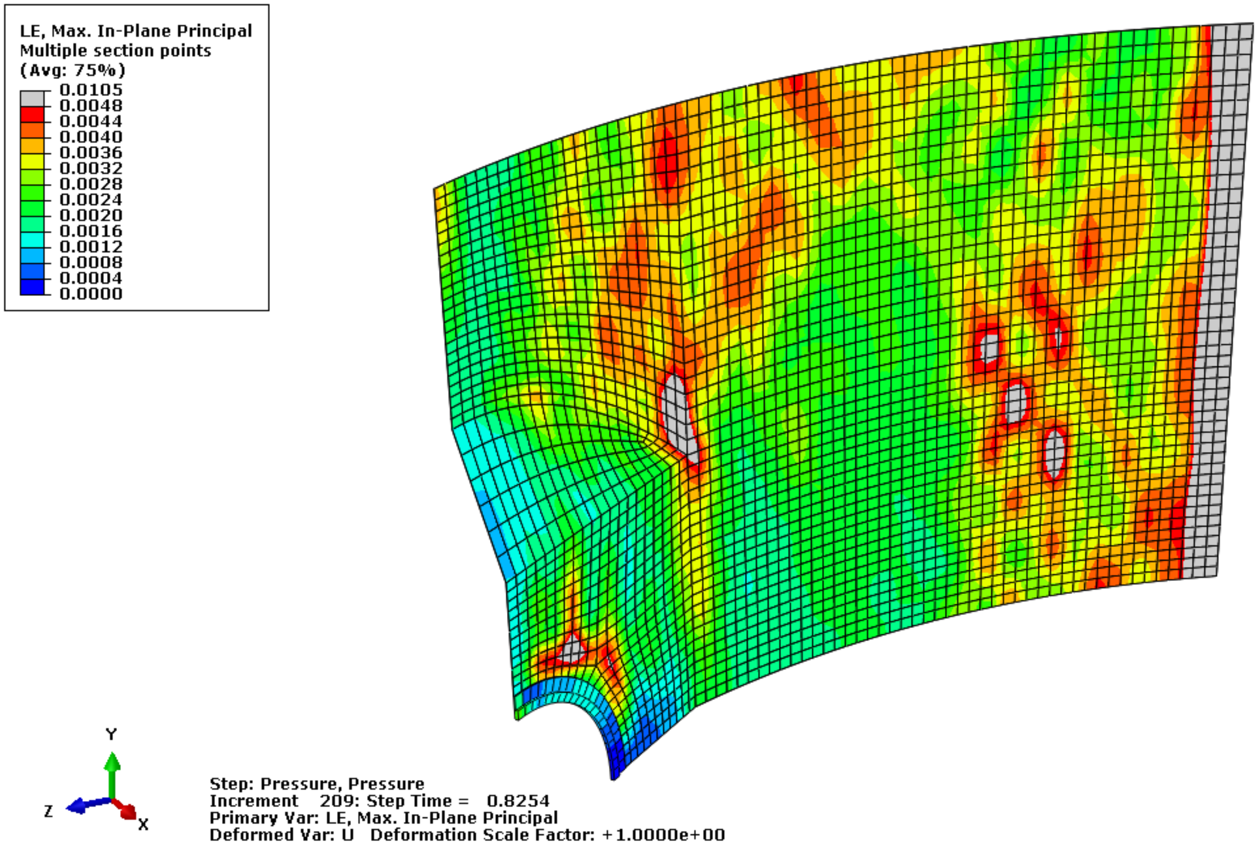

Liner Max Principal Strains at $3.3xP_d$ for Model 2b

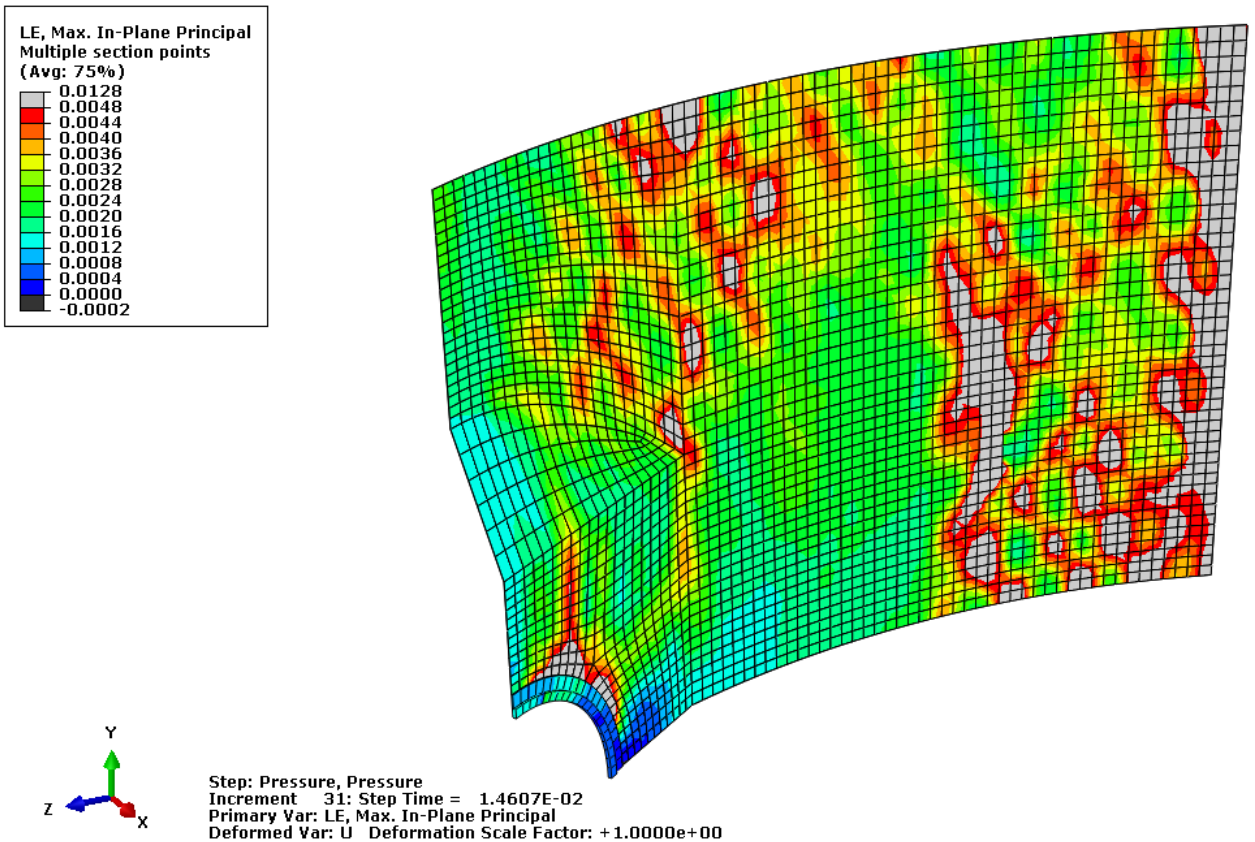

Liner Max Principal Strains at 3.3xP_d for Model 2c

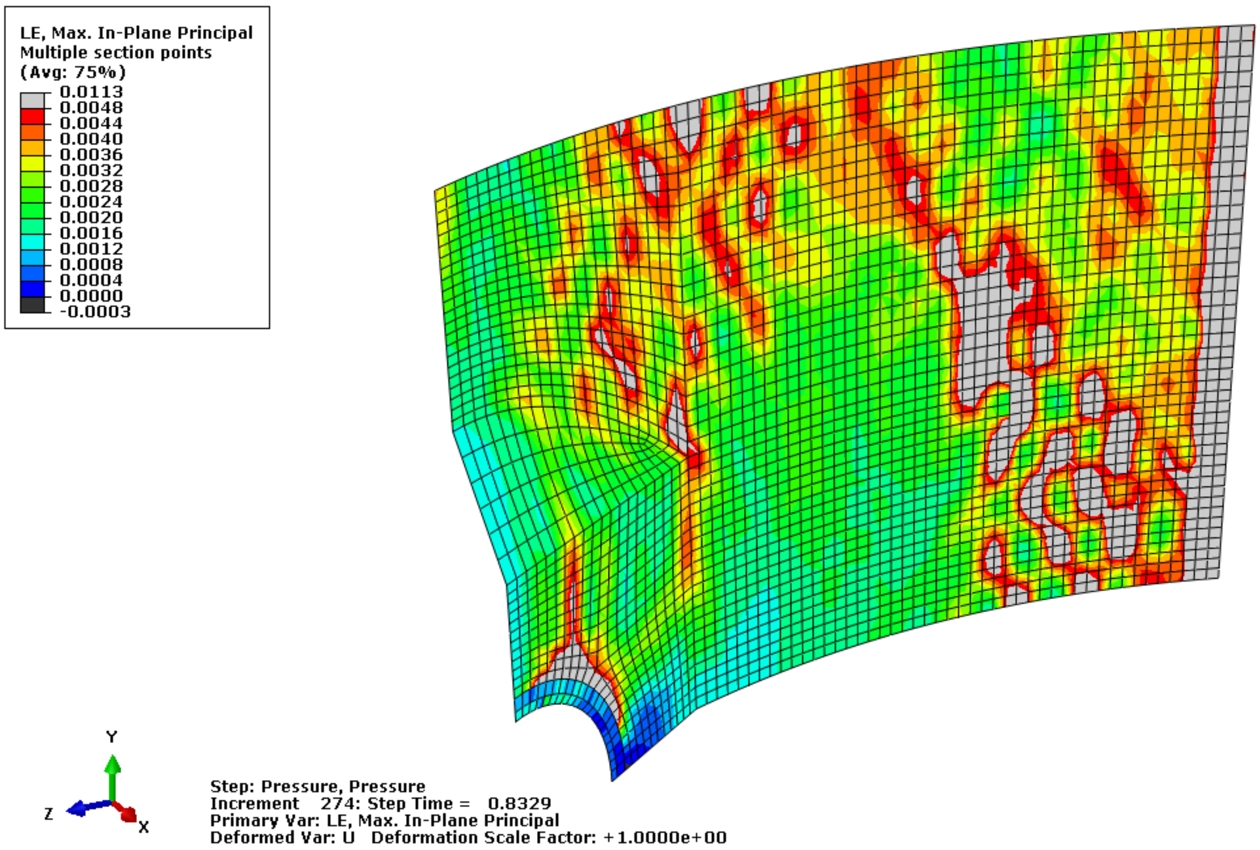

Liner Max Principal Strains at $3.47xP_d$ for Model 2a

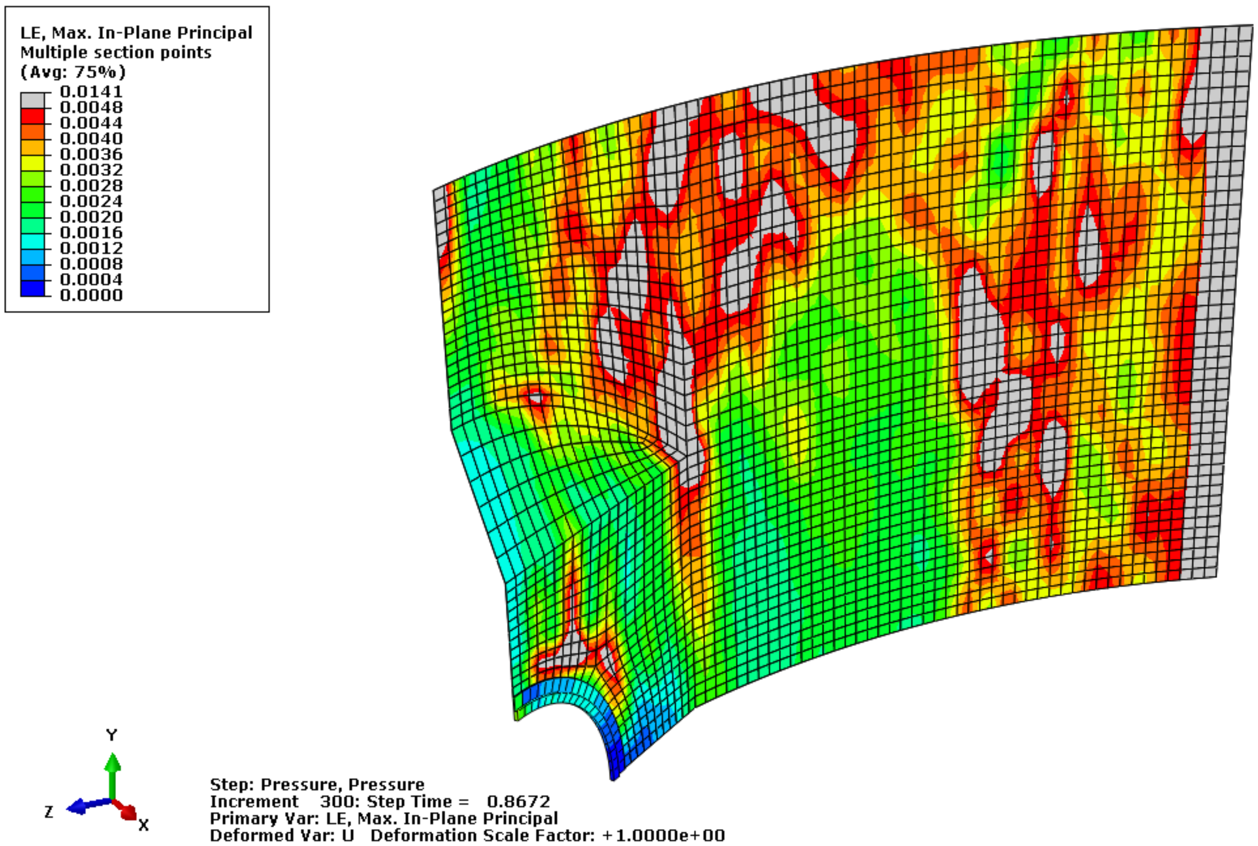

MOFFATT & NICHOL

Sandia National Laboratories

Liner Max Principal Strains at 3.47xP_d for Model 2b

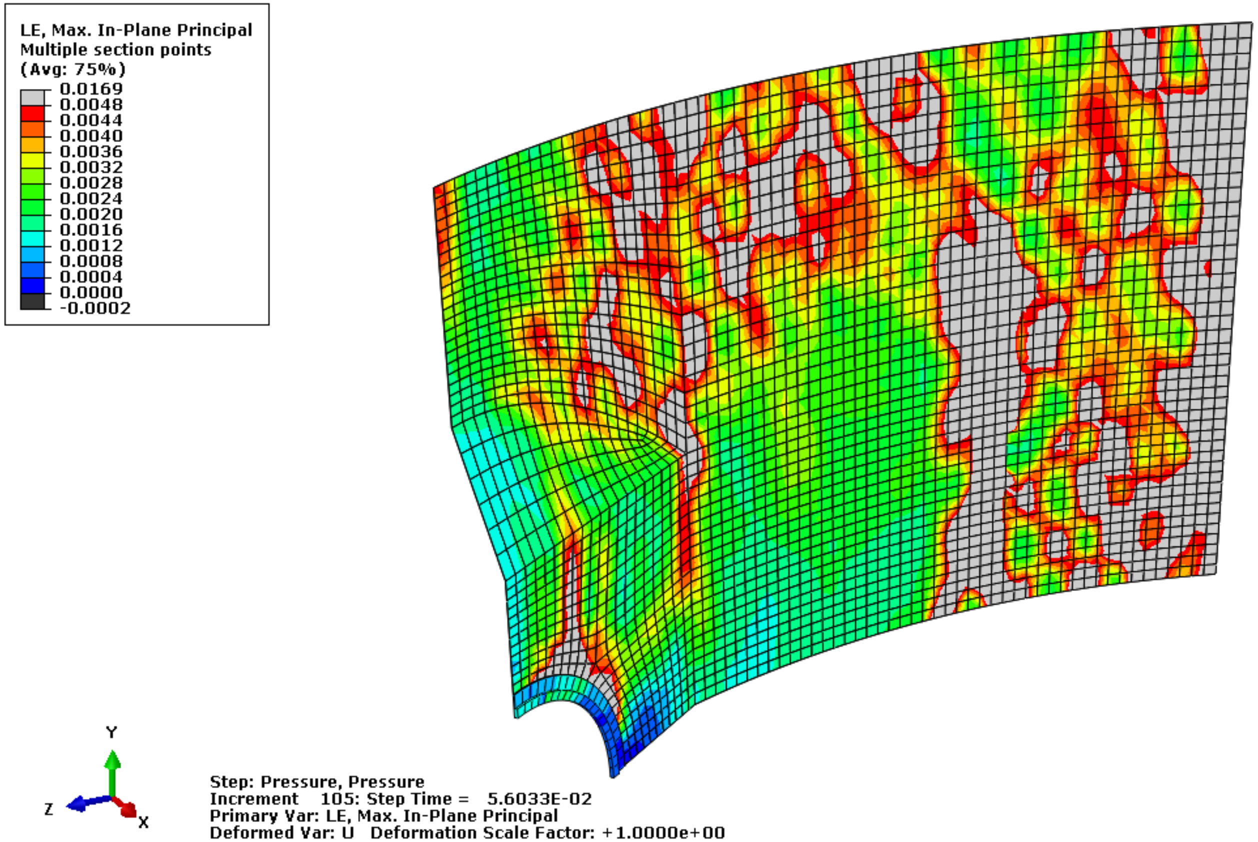

MOFFATT & NICHOL

Sandia National Laboratories

Liner Max Principal Strains at 3.47xP_d for Model 2c

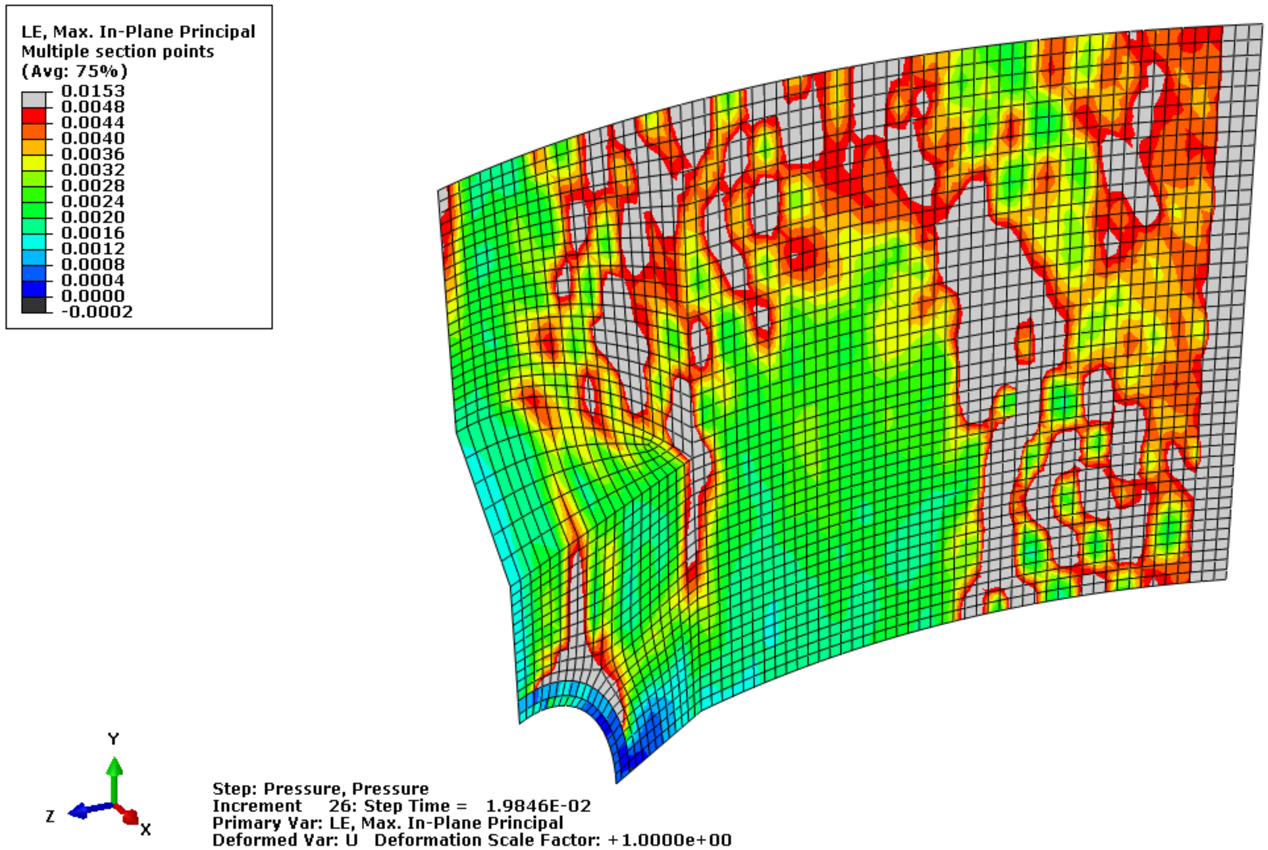

Pipe Separation from Concrete (in) at $2.5xP_d$ for Model 2b

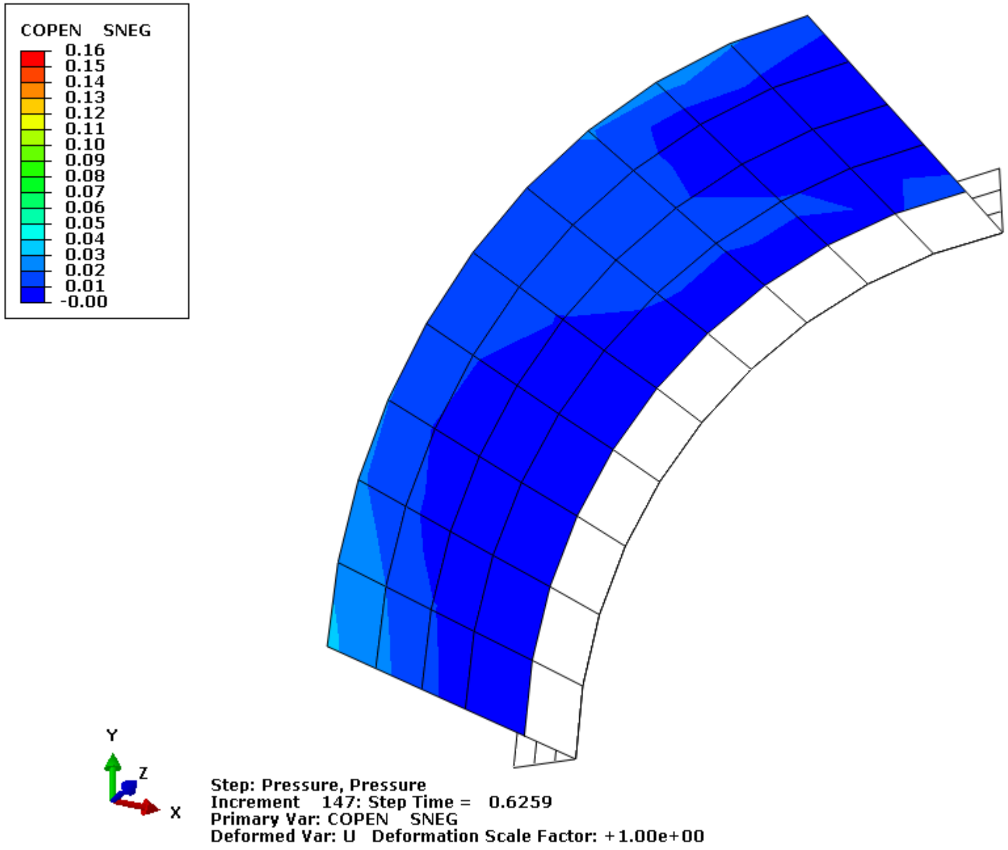

MOFFATT & NICHOL

Sandia National Laboratories

Pipe Separation from Concrete (in) at $3.0xP_d$ for Model 2b

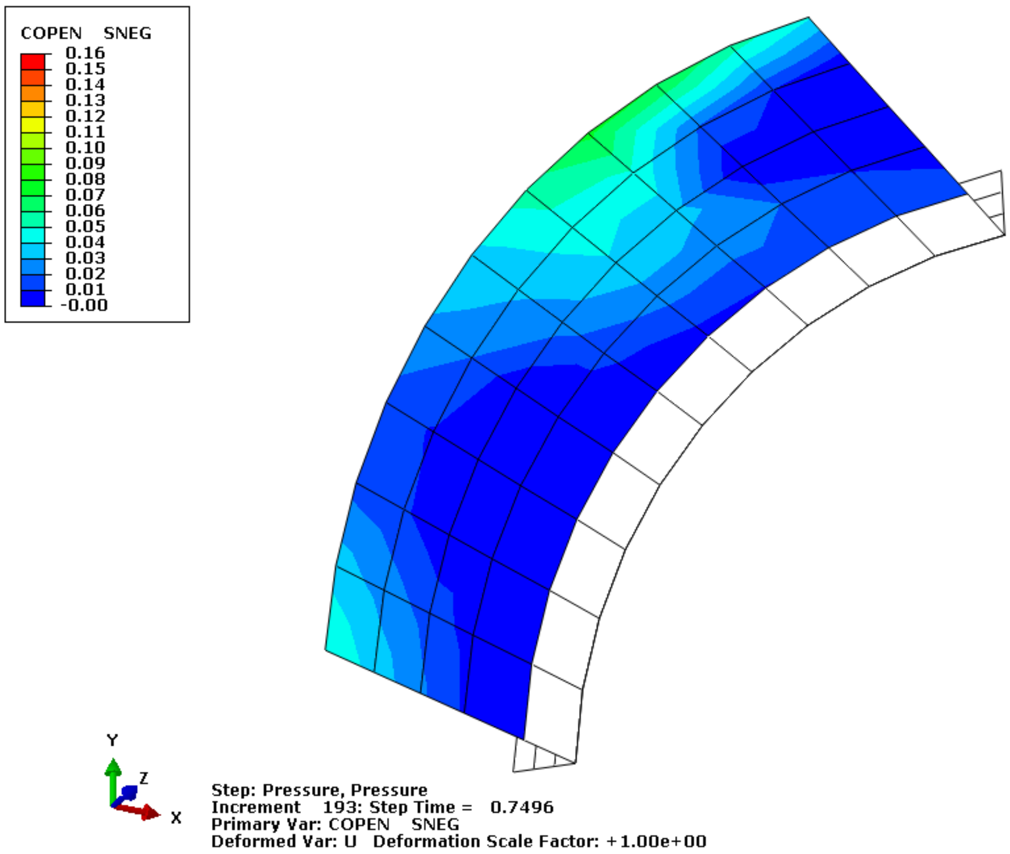

Pipe Separation from Concrete (in) at $3.4xP_d$ for Model 2a

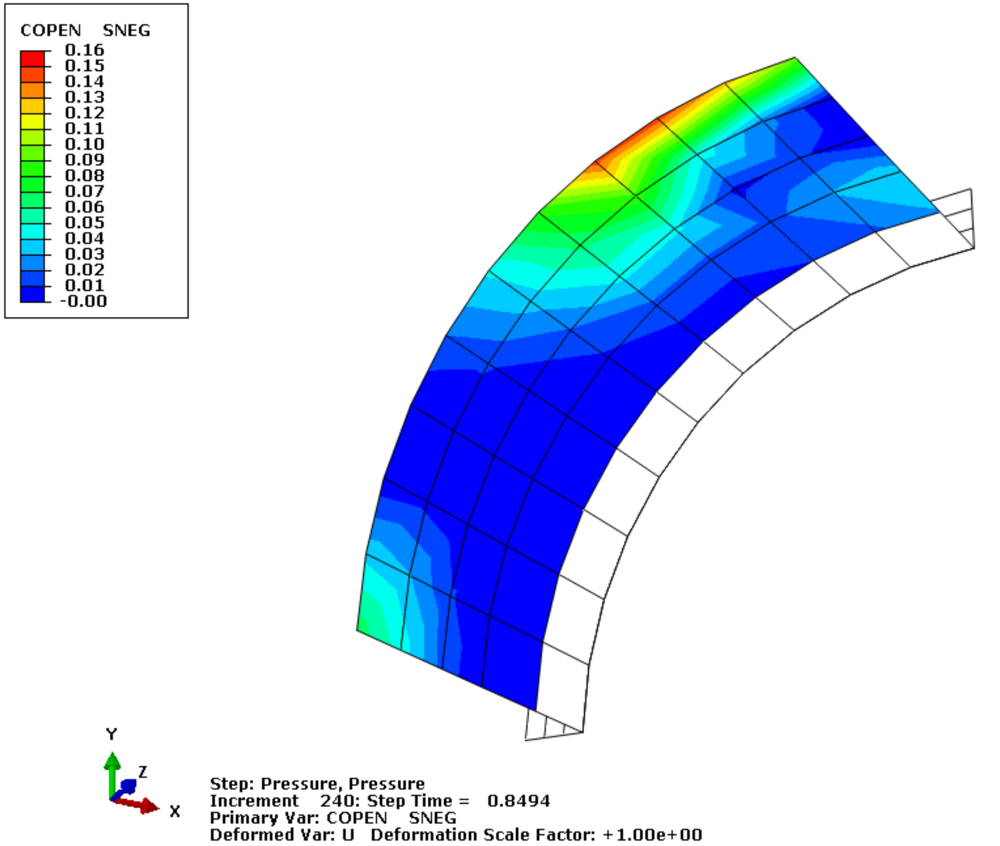

Pipe Separation from Concrete (in) at $3.4xP_d$ for Model 2c

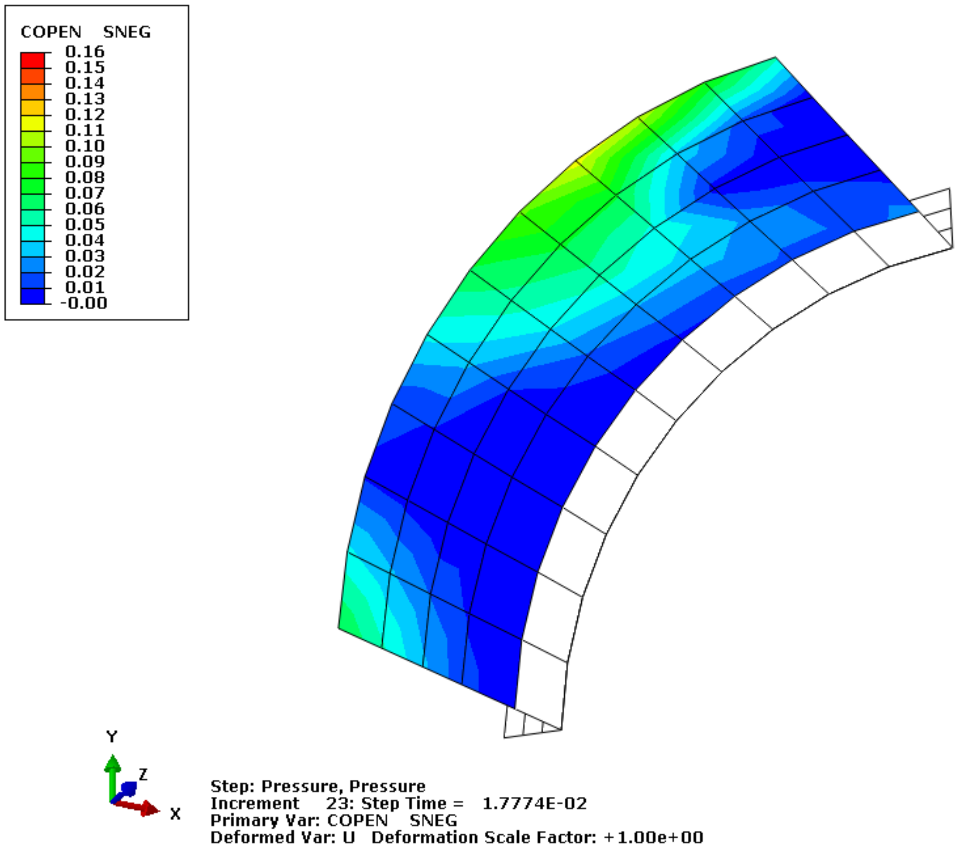

Pipe Separation from Concrete (in) at $3.47xP_d$ for Model 2a

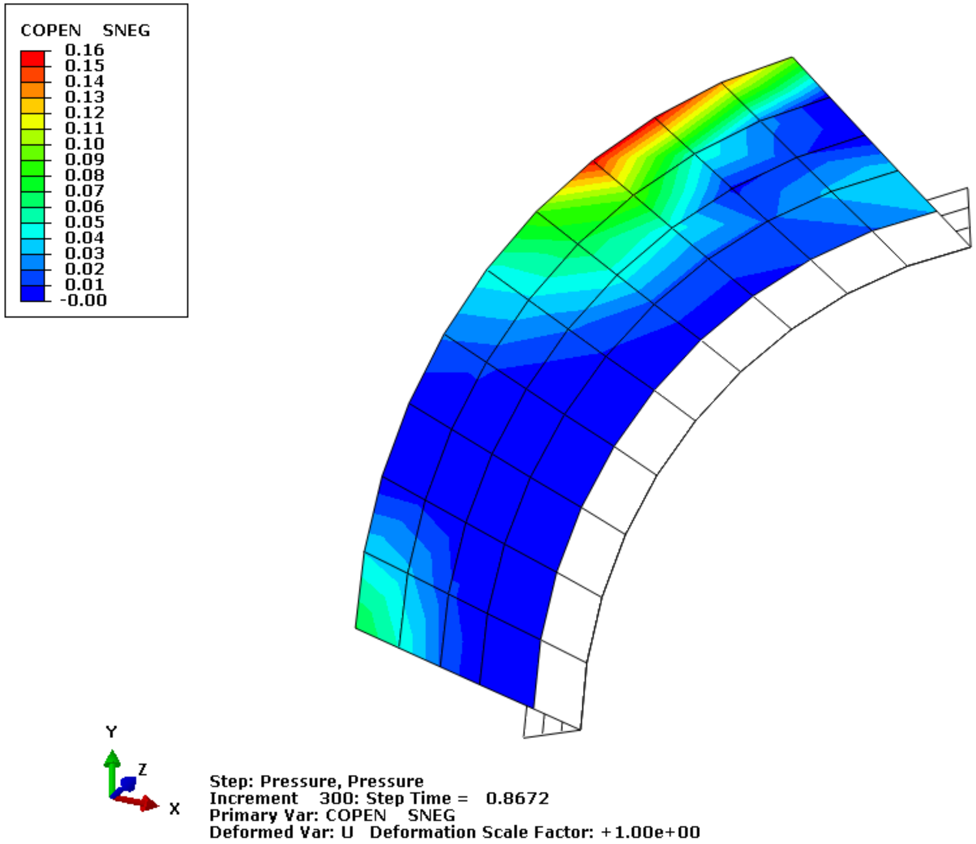

Pipe Separation from Concrete (in) at $3.47xP_d$ for Model 2c

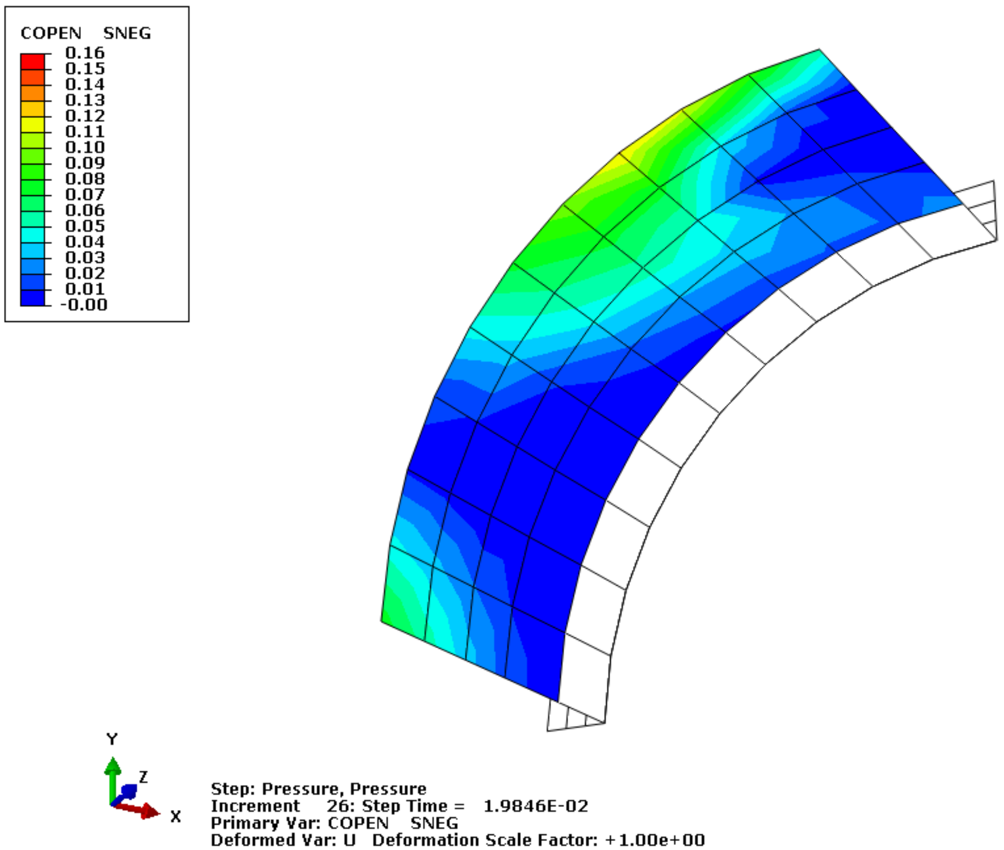

Failure Prediction

- State-of-the-art for predicting tearing for steel shells comprised of plates, weld seams, stiffeners consist of two fundamental types of failure criteria:
  1. Strain-based failure criteria applied to unflawed steel material and components (described earlier)
  2. Fracture-based methods applied to postulated flaws, which are commonly found in welded steel structures
- Both are relevant to PCCV liners, but both have different information requirements
- Failure Criteria Type 2 is more demanding in terms of information required

Failure Prediction

- For PCCVs, it may be a better predictor of “failure” because it guides the prediction of failure size, while Criteria Type 1 does not
- Approximate procedure is needed, or “transfer function” for correlating J-based fracture prediction to strains in PCCV Liner
- Ultimately, this also leads to prediction of liner tear lengths and opening areas versus strain in the liner
- Final step from prediction of J for a typical “flawed” piece of liner, to prediction of specific numbers and sizes of cracks, requires addition of statistical assessment

Crack Modeling for Use in Strain-to-J-Mapping

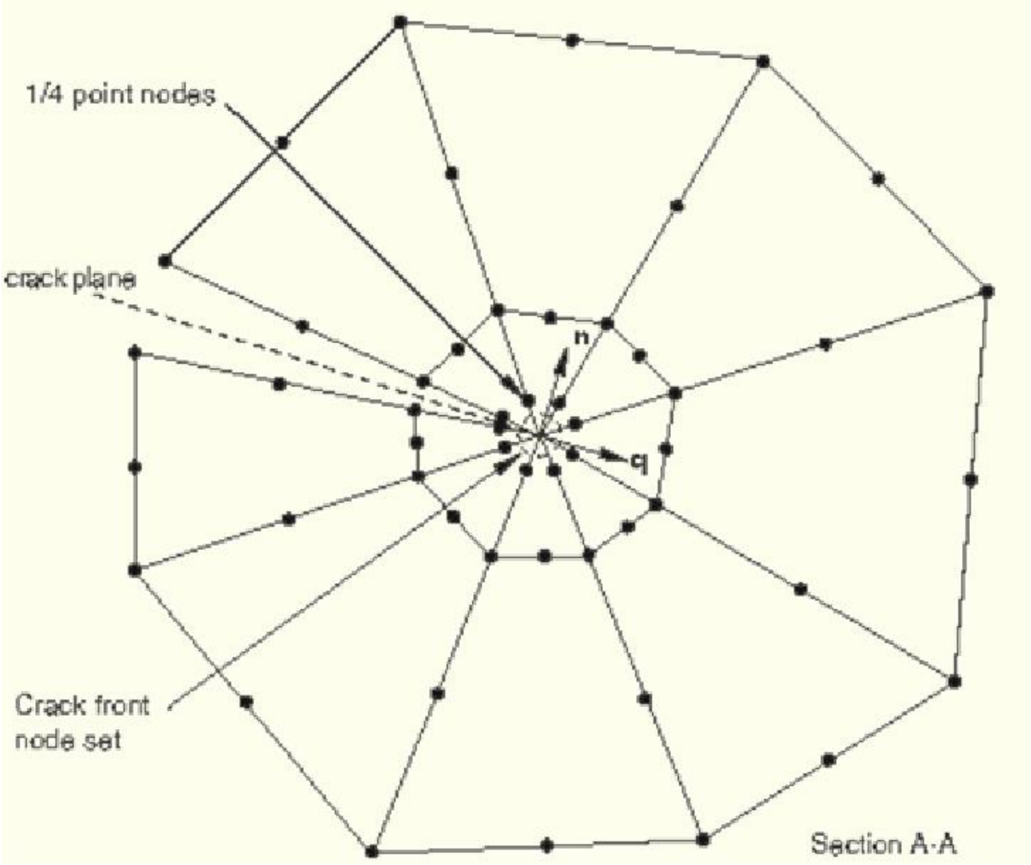

MOFFATT & NICHOL

Sandia National Laboratories

Crack FE Modeling for Development of Strain-to-J Mapping

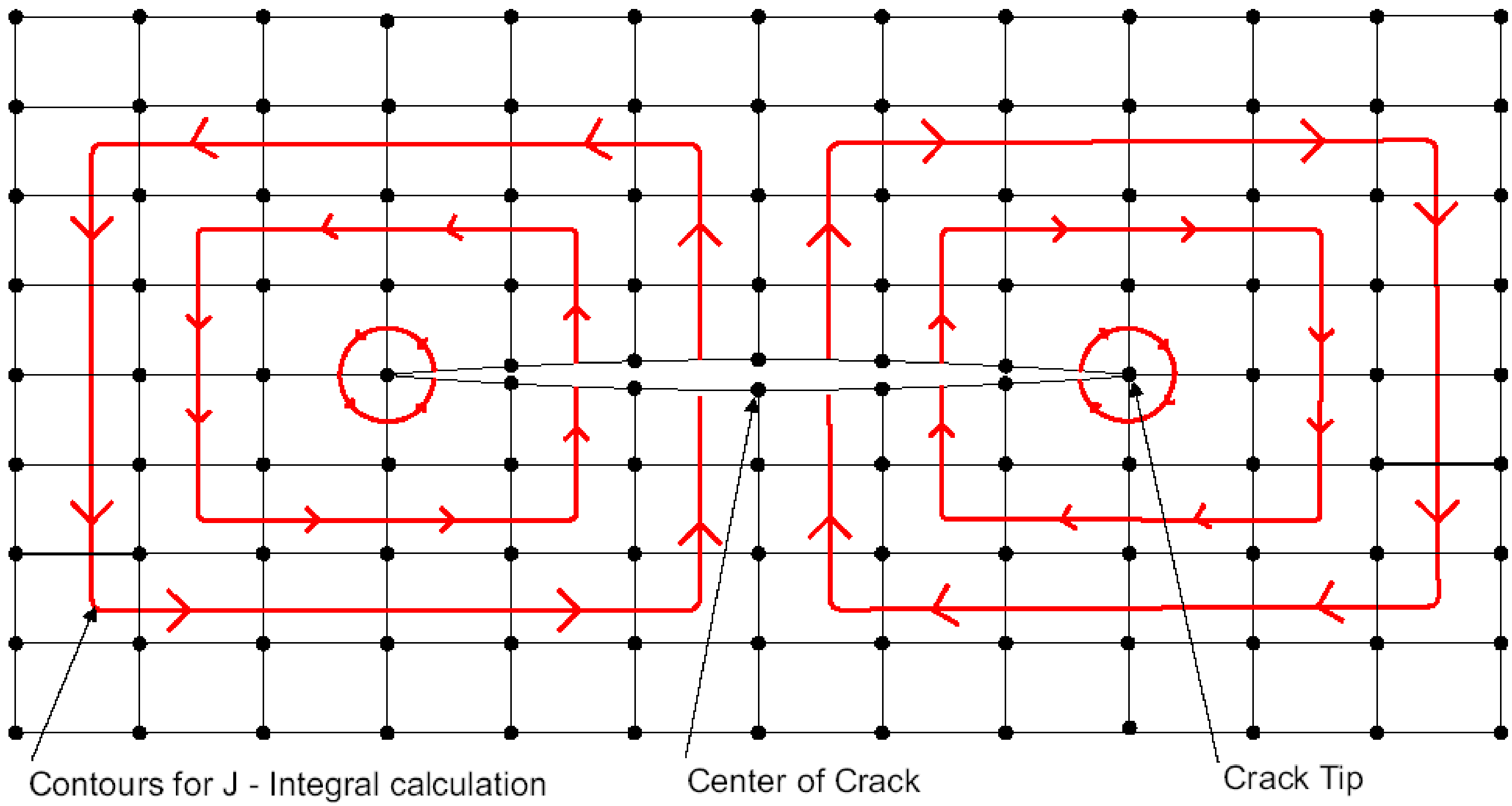

Failure Prediction

- Two fracture models developed as separate FE models with extremely fine mesh (element size of 0.01-inch), appropriate to embedding small initial cracks into the models, calculating J-integrals and propagating cracks
- Fracture models consider two particular conditions where local liner strain concentrations significant – a vertical seam weld, straddled by horizontal stiffener, with or without presence of a vertical T-anchor
- In fracture mechanics work, it is typical to assume a 'flaw' size equal to thickness of material (in our case 1/16")
- Fracture submodels have a standardized length
- In PCCV, it is the length between the liner anchors
- A gage-length for strain mapping should be relatively immune to differences between analysts mesh size in Models 2 or 3
- For Model 2c, largest strains observed at Locations 6, 8, and 1. This tends to agree with observations around the E/H Region. The largest strains (Location 6) are applied to the fracture analyses

Assumed Initial Flawsize in Fracture Mechanics

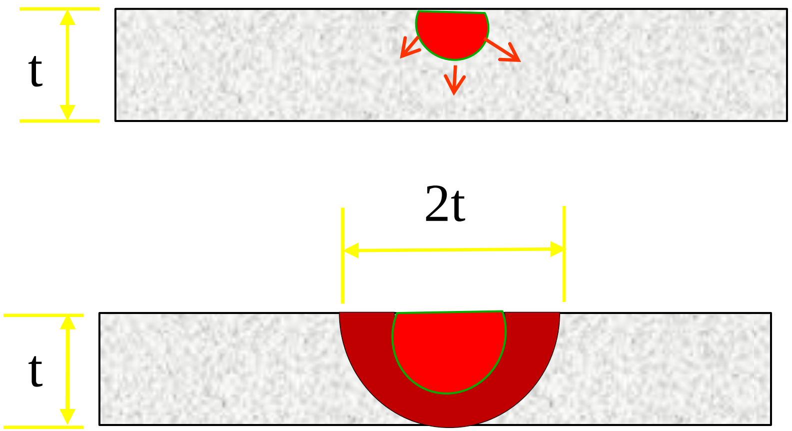

Through Thickness
Crack from Initial Flaw

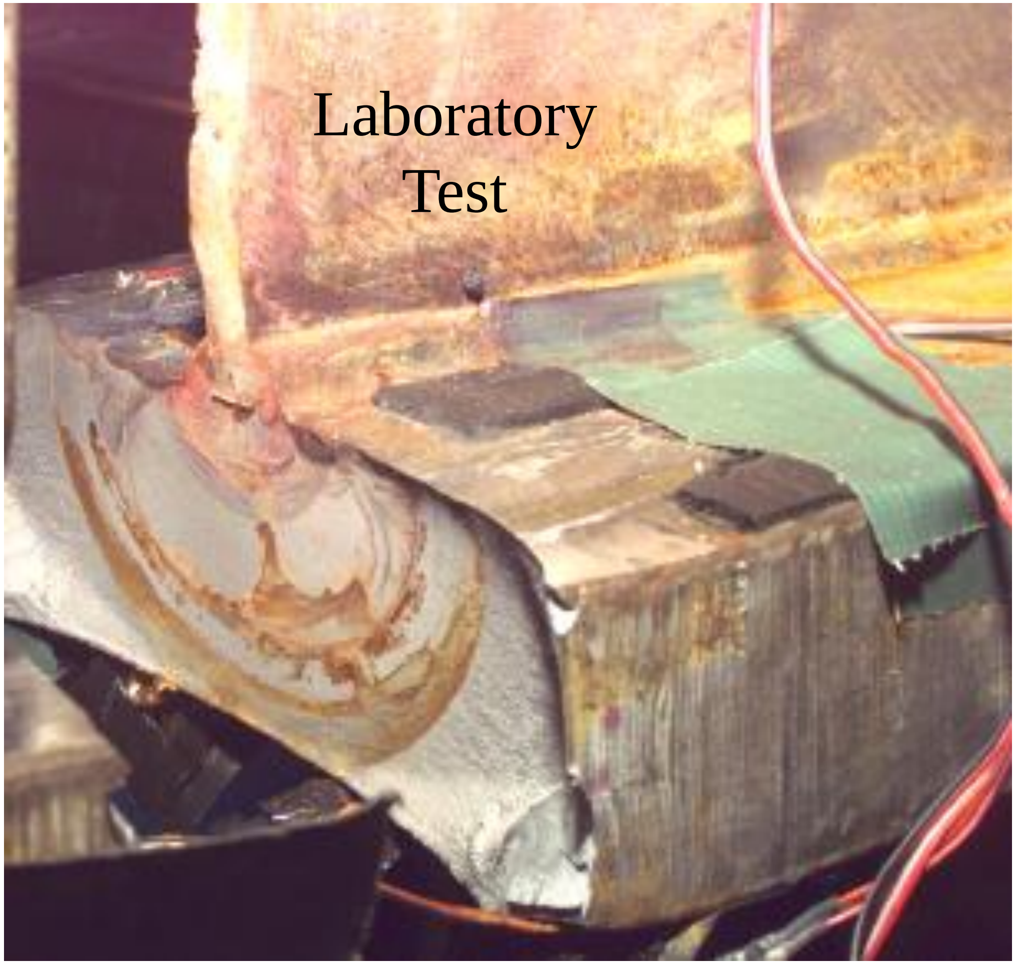

Failure Prediction, cont'd

- Crack propagation threshold needs to be established (but say for example it is J_{cr} = 350 in-lb/in^2); values such as this come from fracture toughness testing
- Typical J_{cr} values for Grade 50 ksi carbon steels can range from 50-100 in-lb/in^2 to as high as 600-800 in-lb/in^2 but based on recent work on another project, J_{cr} = 350 in-lb/in^2 was found to be a reasonable median value
- J_{cr} is reached when the "averaged strain" (between anchors) is 0.0028. This corresponds to a pressure of approximately 2.7xP_d (by cross referencing to the Model 2c Liner Strain graph)
- A small flaw in the liner would first begin to grow (and leak substantially) at a pressure of 2.7xP_d. Conclusion from this is similar to observations made during the PCCV testing
- Such predictions for onset of tearing, AND predictions of the length of tears will be conducted in the Phase 2 work

Dimensions of Fracture Model 1 (same as Fracture Model 2)

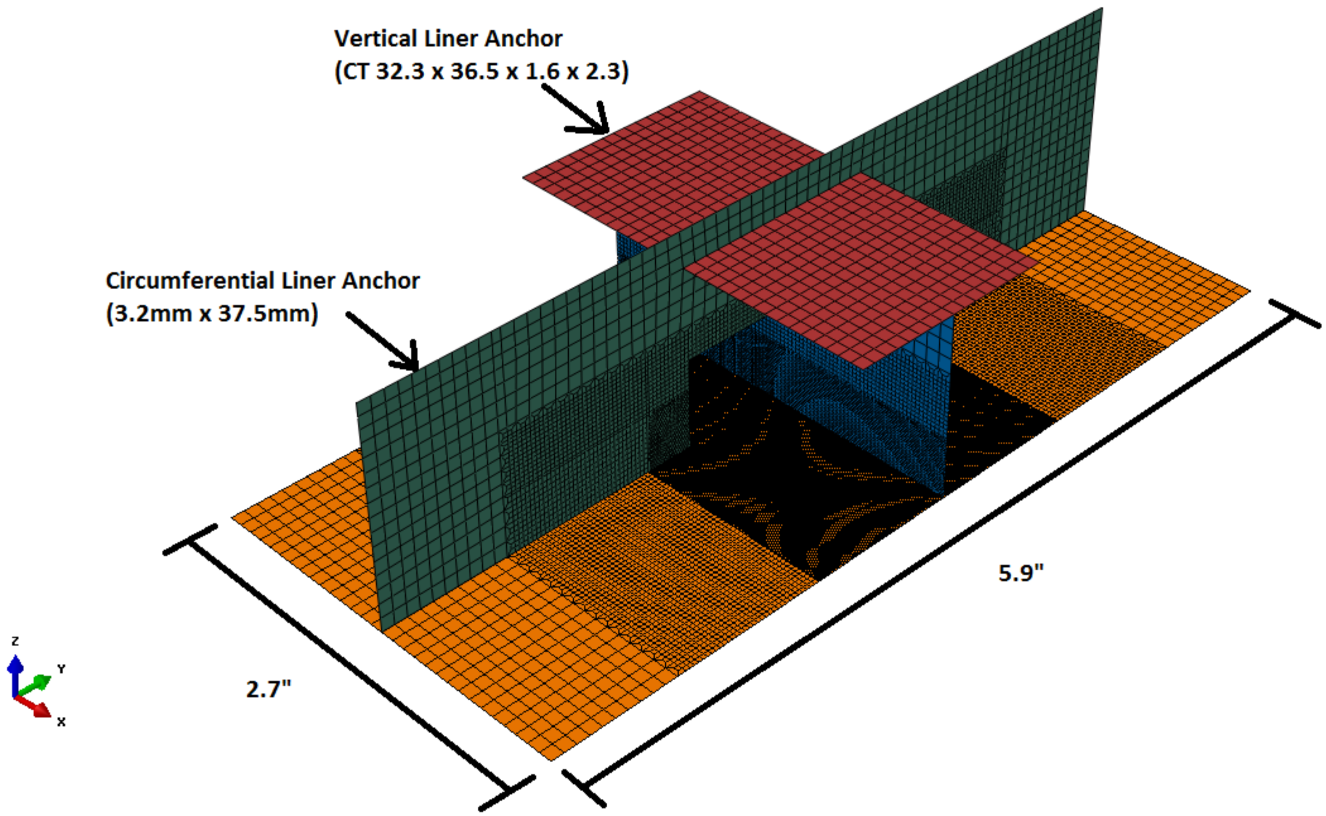

MOFFATT & NICHOL
Sandia National Laboratories

Boundary Conditions Applied to fracture Model (shell thickness rendered)

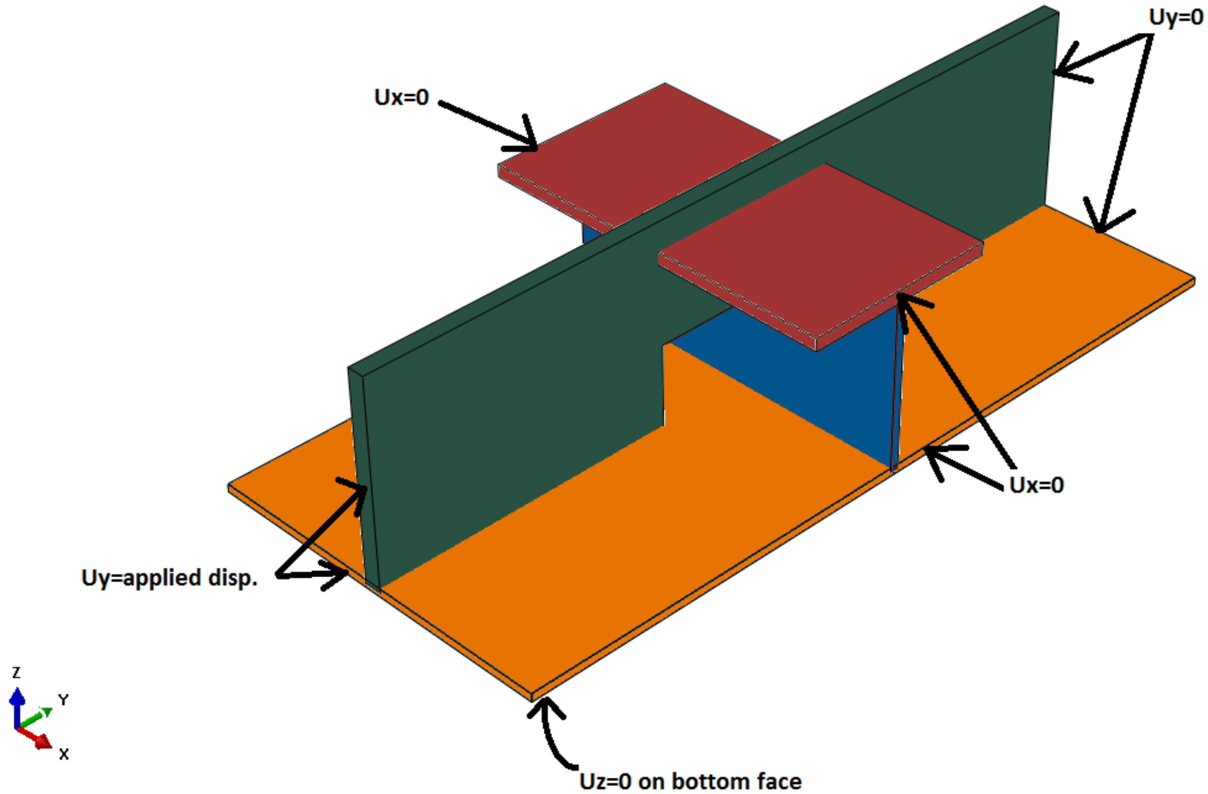

Crack Size and Location on Fracture Model 1

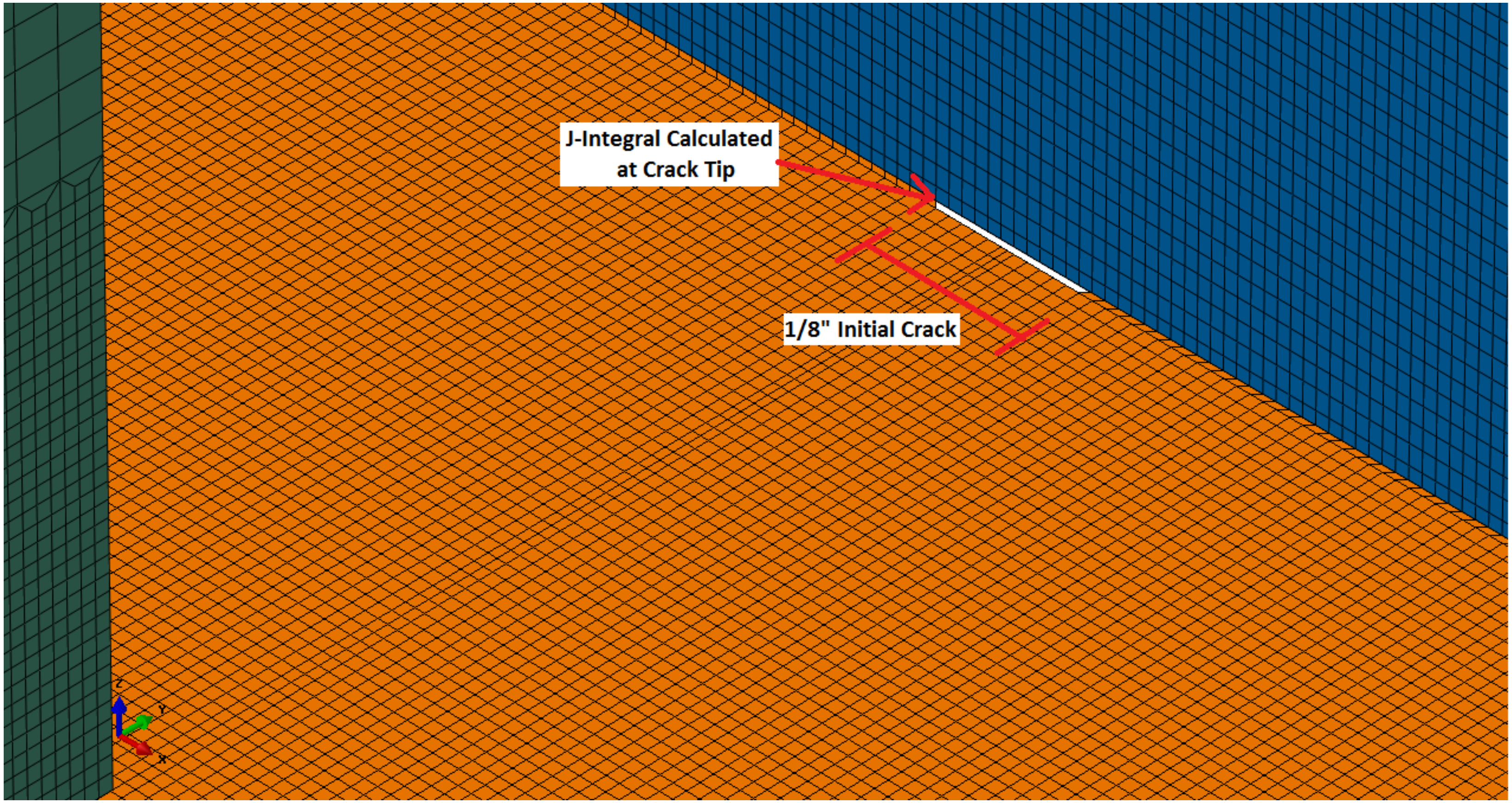

MOFFATT & NICHOL

Sandia National Laboratories

Fracture Model 2 (Same a Fracture Model 1 with Vertical Liner Anchor Removed)

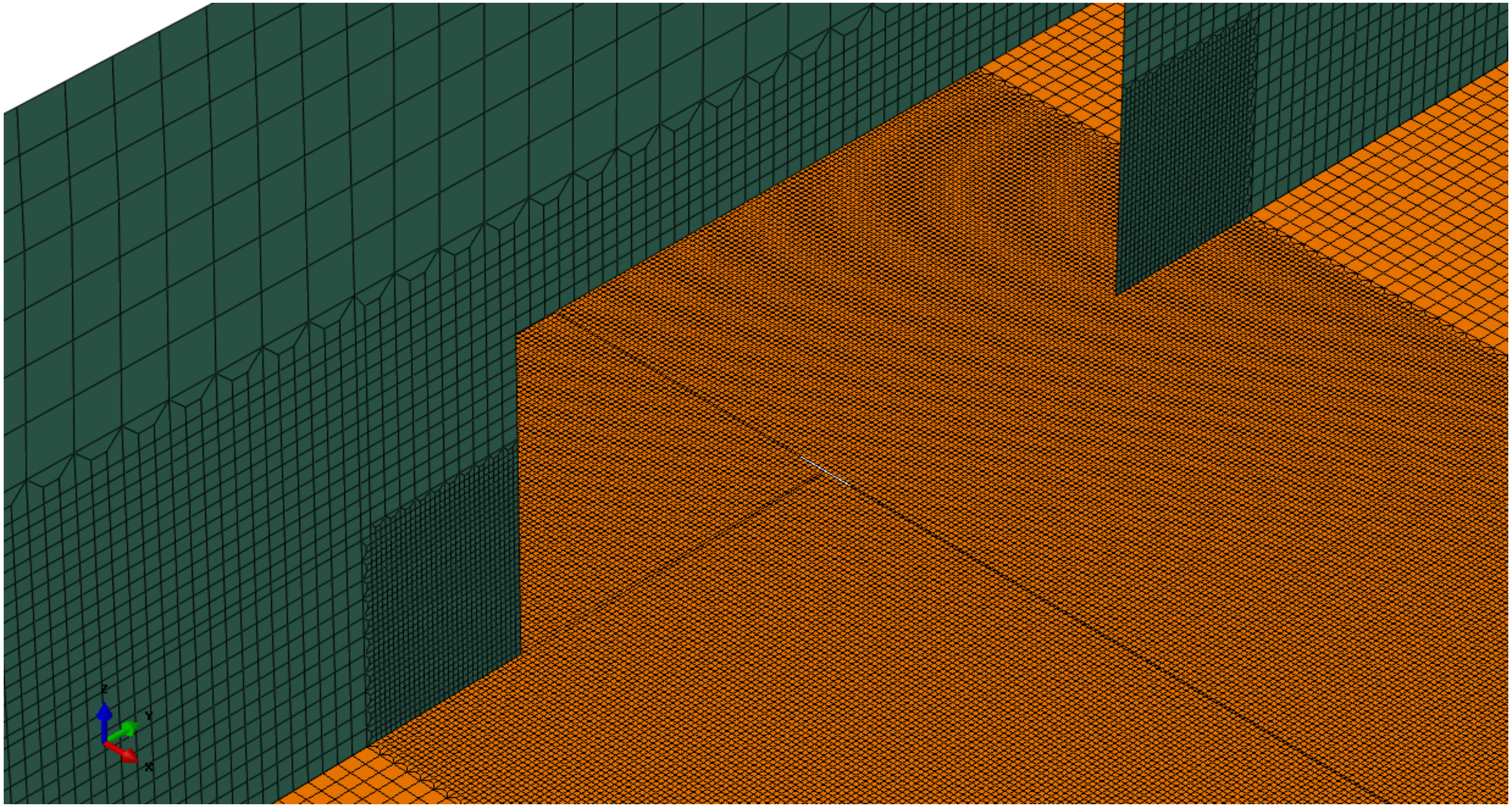

Circumferential Strain at Specified Locations vs. Multiples of Design Pressure for Model 2a

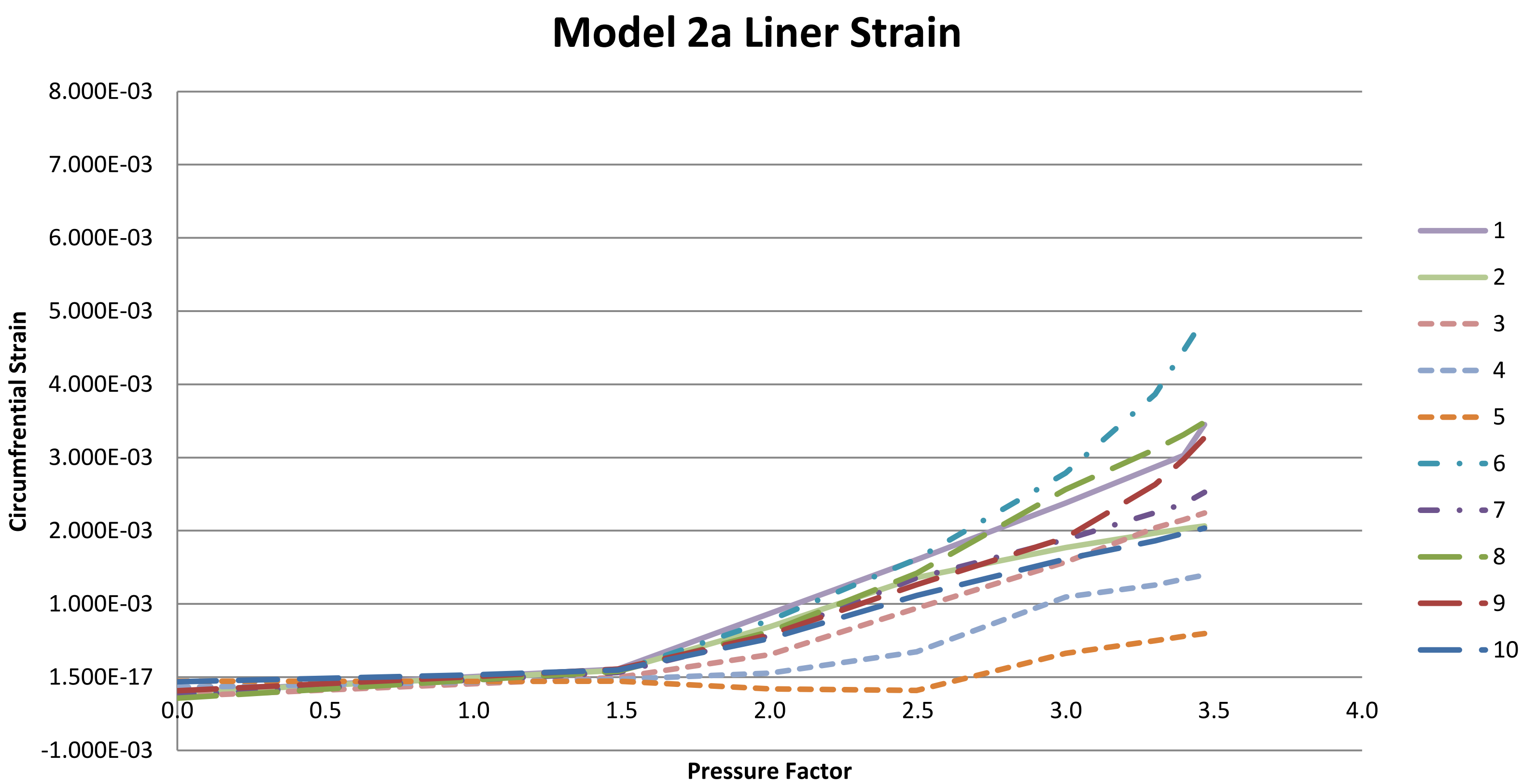

MOFFATT & NICHOL
Sandia National Laboratories

Circumferential Strain at Specified Locations vs. Multiples of Design Pressure for Model 2b

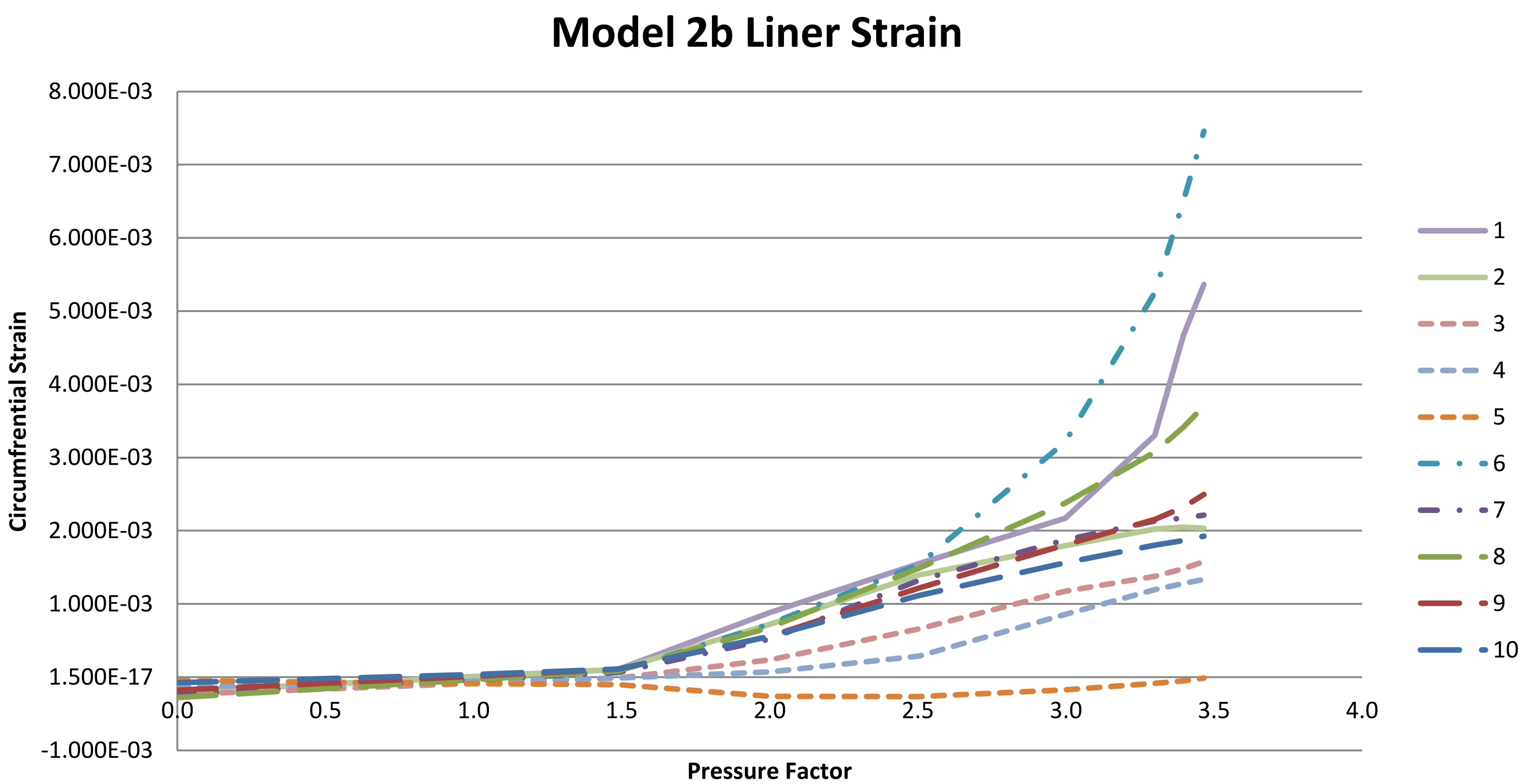

MOFFATT & NICHOL

Sandia National Laboratories

Circumferential Strain at Specified Locations vs. Multiples of Design Pressure for Model 2c

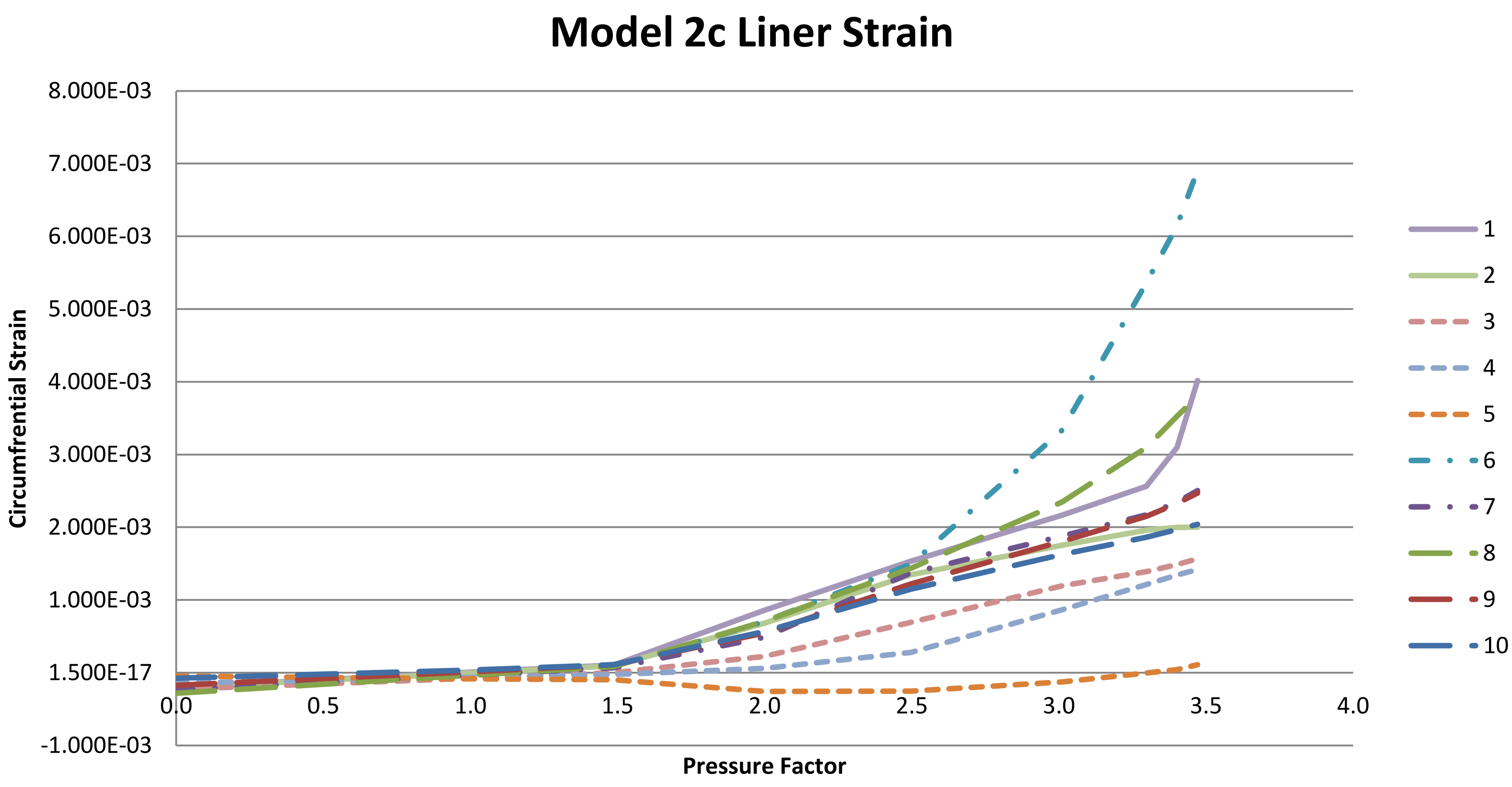

MOFFATT & NICHOL

Sandia National Laboratories

Circumferential Strain in Model 1 with Average Strain of 0.00372

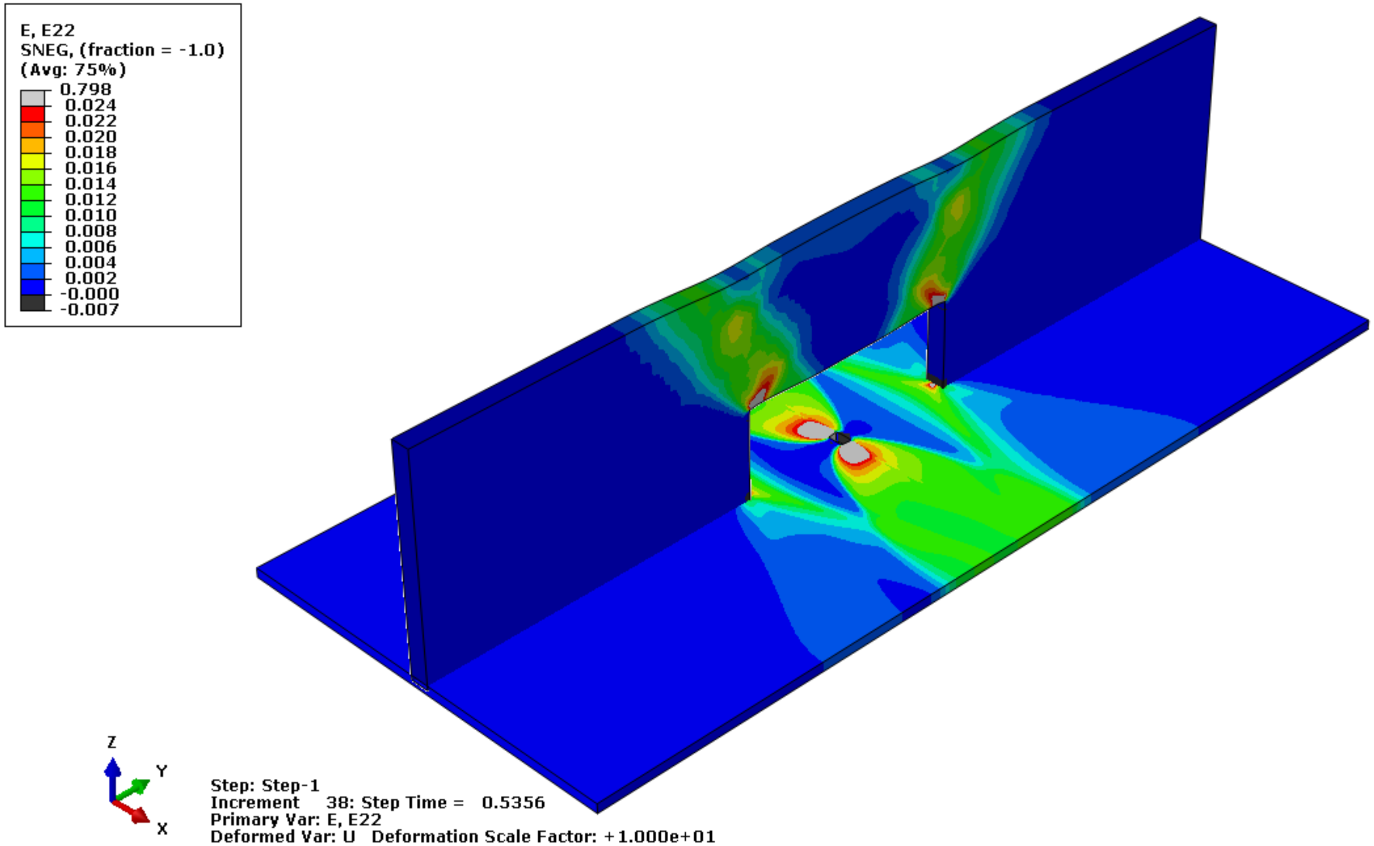

(Vertical Liner Anchor not Displayed for Clarity)

MOFFATT & NICHOL
Sandia National Laboratories

Circumferential Strain in Model 1 with Average Strain of 0.00419

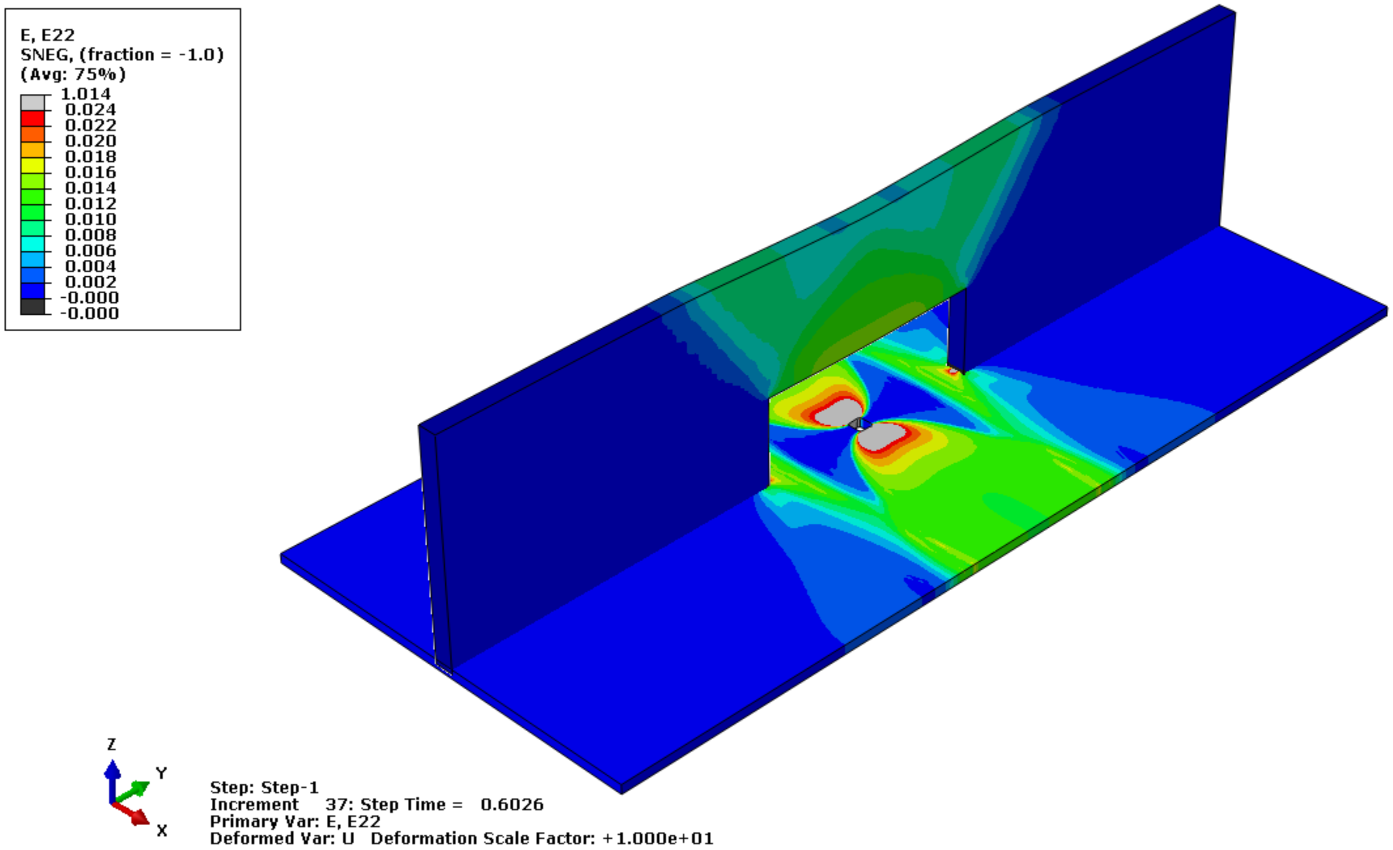

MOFFATT & NICHOL

Sandia National Laboratories

J-integral vs. Circumferential Strain in Fracture Model 1 and 2